[13] M. Ueno, M. Itoh, L. Kong, K. Sugihara, M. Asano, N. Takakura, PSF1 is essential for early embryogenesis in mice, Mol. Cell. Biol. 25 (2005) 10528–10532.
[14] L. Kong, M. Ueno, M. Itoh, K. Yoshioka, N. Takakura, Identification and characterization of mouse PSF1-binding protein, SLD5, Biochem. Biophys. Res. Commun. 339 (2006) 1204–1207.
[15] N. Kimura, M. Ueno, K. Nakashima, T. Taga, A brain region-specific gene product Lhx6.1 interacts with Ldb1 through tandem LIM-domains, J. Biochem. 126 (1999) 180–187.
[16] M. Ueno, N. Kimura, K. Nakashima, F. Saito-Ohara, J. Inazawa, T. Taga, Genomic organization, sequence and chromosomal localization of the mouse Tbr2 gene and a comparative study with Tbr1, Gene 254 (2000) 29–35.
[17] T. Shinohara, K.E. Orwig, M.R. Avarbock, R.L. Brinster, Spermatogonial stem cell enrichment by multiparameter selection of mouse testis cells, Proc. Natl. Acad. Sci. USA 97 (2000) 8346–8351.
[18] N. Takakura, T. Watanabe, S. Suenobu, Y. Yamada, T. Noda, Y. Ito, M. Satake, T. Suda, A role for hematopoietic stem cells in promoting angiogenesis, Cell 102 (2000) 199–209.
[19] S.T. Smale, Transcription initiation from TATA-less promoters within eukaryotic protein-coding genes, Biochim. Biophys. Acta 1351 (1997) 73–88.
[20] N. Dyson, The regulation of E2F by pRB-family proteins, Genes Dev. 12 (1998) 2245–2262.
[21] B.D. Rowland, R. Bernards, Re-evaluating cell-cycle regulation by E2Fs, Cell 127 (2006) 871–874.
[22] U. Steidl, R. Kronenwett, U.P. Rohr, R. Fenk, S. Kliszewski, C. Maercker, P. Neubert, M. Aivado, J. Koch, O. Modlich, H. Bojar, N. Gattermann, R. Haas, Gene expression profiling identifies significant differences between the molecular phenotypes of bone marrow-derived and circulating human CD34+ hematopoietic stem cells, Blood 99 (2002) 2037–2044.
[23] M.L. Mucenski, K. McLain, A.B. Kier, S.H. Swerdlow, C.M. Schreiner, T.A. Miller, D.W. Pietryga, W.J. Scott Jr., S.S. Potter, A functional c-myb gene is required for normal murine fetal hepatic hematopoiesis, Cell 65 (1991) 677–689.
[24] T. Okuda, J. van Deursen, S.W. Hiebert, G. Grosveld, J.R. Downing, AML1, the target of multiple chromosomal translocations in human leukemia, is essential for normal fetal liver hematopoiesis, Cell 84 (1996) 321–330.
[25] P.R. Hoyt, C. Bartholomew, A.J. Davis, K. Yutzey, L.W. Gamer, S.S. Potter, J.N. Ihle, M.L. Mucenski, The Evi1 proto-oncogene is required at midgestation for neural, heart, and paraxial mesenchyme development, Mech. Dev. 65 (1997) 55–70.
[26] H. Iwasaki, K. Akashi, Myeloid lineage commitment from the hematopoietic stem cell, Immunity 26 (2007) 726–740.
[27] F.Y. Tsai, G. Keller, F.C. Kuo, M. Weiss, J. Chen, M. Rosenblatt, F.W. Alt, S.H. Orkin, An early haematopoietic defect in mice lacking the transcription factor GATA-2, Nature 371 (1994) 221–226.
[28] C. Heyworth, K. Gale, M. Dexter, G. May, T. Enver, A GATA-2/estrogen receptor chimera functions as a ligand-dependent negative regulator of self-renewal, Genes Dev. 13 (1999) 1847–1860.
[29] S. Ezoe, I. Matsumura, S. Nakata, K. Gale, K. Ishihara, N. Minegishi, T. Machii, T. Kitamura, M. Yamamoto, T. Enver, Y. Kanakura, GATA-2/estrogen receptor chimera regulates cytokine-dependent growth of hematopoietic cells through accumulation of p21(WAF1) and p27(Kip1) proteins, Blood 100 (2002) 3512–3520.
[30] K. Kitajima, M. Masuhara, T. Era, T. Enver, T. Nakano, GATA-2 and GATA-2/ER display opposing activities in the development and differentiation of blood progenitors, EMBO J. 21 (2002) 3060–3069.
[31] D.A. Persons, J.A. Allay, E.R. Allay, R.A. Ashmun, D. Orlic, S.M. Jane, J.M. Cunningham, A.W. Nienhuis, Enforced expression of the GATA-2 transcription factor blocks normal hematopoiesis, Blood 93 (1999) 488–499.

Both alleles of *PSF1* are required for maintenance of pool size of immature hematopoietic cells and acute bone marrow regeneration

Masaya Ueno,[1] Machiko Itoh,[2] Kazushi Sugihara,[3] Masahide Asano,[3] and Nobuyuki Takakura[1,2]

[1]Department of Signal Transduction, Research Institute for Microbial Diseases, Osaka University, Osaka; [2]Department of Stem Cell Biology, Cancer Research Institute, Kanazawa University, Kanazawa; and [3]Institute for Experimental Animals, Kanazawa University Advanced Science Research Center, Kanazawa, Japan

Hematopoietic stem cells (HSCs) have a very low rate of cell division in the steady state; however, under conditions of hematopoietic stress, these cells can begin to proliferate at high rates, differentiate into mature hematopoietic cells, and rapidly reconstitute ablated bone marrow (BM). Previously, we isolated a novel evolutionarily conserved DNA replication factor, *PSF1* (*partner of SLD5-1*), from an HSC-specific cDNA library. In the steady state, PSF1 is expressed predominantly in CD34$^+$KSL (c-kit$^+$/Sca-1$^+$/Lineage$^-$) cells and progenitors, whereas high levels of PSF1 expression are induced in KSL cells after BM ablation. In 1-year-old *PSF1*$^{+/-}$ mice, the pool size of stem cells and progenitors is decreased. Whereas young *PSF1*$^{+/-}$ mutant mice develop normally, are fertile, and have no obvious differences in hematopoiesis in the steady state compared with wild-type mice, intravenous injection of 5-fluorouracil (5-FU) is lethal in *PSF1*$^{+/-}$ mice, resulting from a delay in induction of HSC proliferation during ablated BM reconstitution. Overexpression studies revealed that PSF1 regulates molecular stability of other GINS components, including SLD5, PSF2, and PSF3. Our data indicate that PSF1 is required for acute proliferation of HSCs in the BM of mice. (Blood. 2009;113:555-562)

Introduction

Tissue regeneration is one of the most tightly controlled processes requiring an ordered program involving induction of proliferation and differentiation of damaged-tissue stem cells. In the normal state, hematopoietic stem cells (HSCs) undergo cell division at a very low rate. However, if the bone marrow (BM) is ablated by an anticancer drug or radioactivity, HSCs that are in a quiescent state are stimulated to proliferate and restore the BM; self-renewal of HSCs is involved in this process.[1] In a mouse experimental model, only one HSC was found to be sufficient to reconstitute the entire hematopoiesis.[2] In this system, it has been suggested that daughter cells derived from HSCs can either commit to a program of differentiation that will eventually result in production of mature, nonproliferating cells or retain HSC properties.

Several proteins thought to be involved in HSCs for induction of self-renewal, including Wnt and Notch ligand families, have been isolated[3-5]; however, what lies downstream of them in the signaling pathway, especially molecules involved in DNA replication, is not known.

PSF1 (partner of SLD5-1) is evolutionarily conserved and is involved in DNA replication in lower eukaryotes,[6-8] and human.[9] PSF1 forms a tetrameric complex (GINS complex) with SLD5, PSF2, and PSF3. Recently, crystal structure of the human GINS complex was reported.[10-13] In yeast, GINS complex associates with MCM2-7 complex and CDC45, and this C-M-G complex (CDC45-MCM2-7-GINS) regulates both the initiation and progression of DNA replication.[14-17]

Previously, we cloned the mouse ortholog of *PSF1* from an HSC-specific cDNA library.[18] *PSF1* is predominantly expressed in highly proliferative tissues, such as testis and BM. Loss of *PSF1* causes embryonic lethality around the implantation stage.[18] *PSF1*$^{-/-}$ embryos revealed impaired proliferation of multipotent stem cells, ie, the inner cell mass. In mice, *PSF1* is highly expressed in proliferating HSCs and the hematopoietic progenitor cells (HPCs). However, the biologic function of PSF1 in hematopoiesis is not understood.

In this study, we used *PSF1*$^{+/-}$ mice for studying the function of PSF1 in hematopoiesis. Here we show that haploinsufficiency of *PSF1* causes loss of regeneration capacity resulting from a delay in induction of acute proliferation of HSCs after BM ablation. Our data suggest that both alleles of *PSF1* are essential for acute proliferation of HSCs after BM ablation.

Methods

Mice

C57BL/6 mice were purchased from SLC (Shizuoka, Japan). *PSF1* mutant mice and *Runx1*-deficient mice (*Runx1*-deficient mice were a gift from Dr T. Watanabe, Tohoku University, Sendai, Japan) were maintained and bred as described.[18,19] All animal studies were approved by the Animal Care Committee of Kanazawa University and the Osaka University Animal Care and Use Committee. For BM ablation studies, 8-week-old wild-type and *PSF1*$^{+/-}$ mice were treated with a single tail vein injection of 5-fluorouracil (5-FU; 150 mg/kg body weight; Kyowa Hakko Kogyo, Tokyo, Japan).

Immunohistochemistry and FACS analysis

Tissue fixation, preparation of tissue sections, and staining of sections with antibodies were performed as described previously.[18] For immunohistochemistry of fetal liver (FL), rabbit anti-PSF1 antibody was used.[18] Horseradish

Submitted January 29, 2008; accepted September 7, 2008. Prepublished online as *Blood* First Edition paper, November 4, 2008; DOI 10.1182/blood-2008-01-136879.

The online version of this article contains a data supplement.

The publication costs of this article were defrayed in part by page charge payment. Therefore, and solely to indicate this fact, this article is hereby marked "advertisement" in accordance with 18 USC section 1734.

peroxidase-conjugated secondary antibodies were obtained from Jackson ImmunoResearch Laboratories (West Grove, PA). For immunocytochemistry, we used monoclonal anti-PSF1 antibody (Aho57.2; see next paragraph below) as a first antibody and Alexa 488–conjugated antirat IgG (Invitrogen, Carlsbad, CA) as a second antibody. Stained cells and the sections were observed using an Olympus IX-70 microscope equipped with UPlanFl 4/0.13 and LCPlanFl 20 /0.04 dry objective lenses (Olympus, Tokyo, Japan). Images were acquired with a CoolSnap digital camera (Roper Scientific, Trenton, NJ), and processed with Adobe Photoshop version 8.0.1 software (Adobe Systems, San Jose, CA).

For the generation of monoclonal anti-PSF1 antibodies, cDNA encoding the full-length protein sequence of PSF1 was amplified by polymerase chain reaction (PCR), and then cDNA was ligated into pGEX-4T-1 vector (GE Healthcare, Little Chalfont, United Kingdom) for the preparation of glutathione S-transferase (GST)–fusion proteins. PSF1-coding region was amplified from the mouse NIH3T3 cDNA using the primers 5′-GGA ATT CAT GTT CTG CGA AAA AGC TAT G-3′ (sense) and 5′-GGA ATT CTC AGG ACA GCA CGT GCT CTA GA-3′ (antisense) and was subsequently subcloned as a *Eco*RI-*Eco*RI fragment into the pGEX-4T-1 vector (GE Healthcare) in the correct reading frame to express the GST-PSF1 fusion protein. This construct was transformed into *Escherichia coli* JM109 strains (Toyobo Engineering, Osaka, Japan) to obtain GST-tagged fusion proteins. Recombinant GST-PSF1 was purified using glutathione-Sepharose 4B column (GE Healthcare) according to the manufacturer's instructions. Purified GST-fused proteins were used as antigen for immunization of rats, and rat/mouse hybridomas were established by standard procedures.[20] A stable hybridoma cell line, aho57.2, was obtained. The specificities of all antibodies were determined by immunoblotting and immunocytochemistry.

Preparation of FL and BM cells and fluorescence-activated cell sorter (FACS) analysis was as described previously.[21,22] The antibodies used in flow cytometric analysis for lineage marker (Lin) were fluorescein isothiocyanate– or phycoerythrin-conjugated Gr-1 (RB6-8C5), Mac-1 (M1/70), B220 (RA3-6B2), TER119, anti-CD4 (GK1.5), and anti-CD8 (53-6.72). Allophycocyanin-conjugated anti–c-kit (ACK2), and biotin-conjugated anti–Sca-1 and CD34 were also applied. Biotinylated anti–Sca-1 or CD34 was visualized with peridinin chlorophyll protein–streptavidin. These antibodies were purchased from BD Biosciences (San Jose, CA). The stained cells were analyzed by FACSCalibur (BD Biosciences) and sorted by JSAN (Bay Bioscience, Kobe, Japan). For immunocytochemistry of HSCs from 5-FU–treated BM, 300 CD34$^+$ KSL cells were isolated by sorting from BM obtained from 5 mice 4 days after 5-FU treatment. The average number of total BM mononuclear cells and CD34$^+$ KSL obtained from right and left femurs and tibias after treatment with 5-FU was 9.3 plus or minus 5.3×10^6 and 60 plus or minus 38, respectively.

For the analysis of apoptosis, cells were stained with anti–annexin V antibodies (eBioscience, San Diego, CA). For platelet analysis, blood from wild-type and mutant mice was obtained from the tail vein and collected in phosphate-buffered saline (PBS) containing 3.8 mM citric acid, 7.5 mM trisodium citrate, and 10 mM of dextrose (PBS–acid-citrate-dextrose). Cells were stained with fluorescein isothiocyanate–conjugated anti-CD41 antibody (eBioscience).

qRT-PCR

Total RNA was isolated using the RNAeasy Kit (QIAGEN, Valencia, CA) according to the manufacturer's instructions. RNA was reverse transcribed using the ExScript RT Reagent Kit (Takara, Kyoto, Japan). Quantitative reverse-transcription polymerase chain reaction (qRT-PCR) was performed using Platinum SYBR Green qPCR SuperMix-UDG (Invitrogen) on an Mx3000 system (Stratagene, La Jolla, CA). Levels of the specific amplified cDNAs were normalized to the level of glyceraldehydes-3-phosphate dehydrogenase (*GAPDH*) housekeeping control cDNA. We used the following primer sets: 5′-GAA GGG CTC ATG ACC ACA GT-3′ and 5′-GGA TGC AGG GAT GAT GTT CT-3′, for *GAPDH*, and 5′-CCG GTT GCT TCG GAT TAG AG-3′ and 5′-CTC CCA GCG ACC TCA TGT AA-3′ for *PSF1*.

Cell culture

The colony formation unit in culture (CFU-c) assay was performed as described previously.[21] A total of 2×10^2 KSL-Mac-1$^{-/lo}$ cells that had been sorted from the BM of wild-type or *PSF1*$^{+/-}$ mice were placed in 1 mL semisolid medium (MethoCult; StemCell Technologies, Vancouver, BC). After 10 days of culture, the number of colonies was counted.

For the analysis of sensitivity of HSCs to 5-FU, 10^3 KSL cells derived from wild-type or *PSF1*$^{+/-}$ mice were seeded onto semisolid medium and continuously cultured for 10 days with or without 5-FU (1 ng/mL to 1 μg/mL). Each condition was represented by at least 3 wells, and each experiment was performed in triplicate. To examine the number of apoptotic cells in the population of colony-forming cells, colonies grown in methylcellulose semisolid medium were harvested 6 days after the CFU-c assay was initiated, and the cells were stained with Cy5-conjugated anti–annexin V antibody (eBioscience).

Cell-cycle analysis

Cells were sorted by FACS and fixed in 70% ethanol overnight. After treatment with RNase A (0.5 mg/mL; Sigma-Aldrich, St Louis, MO), cells were labeled with 5 μg/mL propidium iodide (PI) and analyzed by FACSCalibur.

Transfection and immunoblot analysis

NIH3T3 cells were transfected with pEF-BOSE, pEF-flag-PSF1, pEF-Myc-SLD5, pEF-HA-PSF2, and/or pEF-VSVG-PSF3, and immunoblotting was performed as previously described.[23] GAPDH was detected with anti-GAPDH antibodies (Chemicon International, Temecula, CA) for endogenous protein control. Transfection efficiency of each plasmid was determined by qRT-PCR (see "qRT-PCR"). We used the following primer sets: 5′-ATG GAC TAC AAG GAC GAC GAT GAC-3′ and 5′-CTC CCA GCG ACC TCA TGT AA-3′ (for *FLAG-PSF1*); 5′-GAG ATG AAC CGA CTT GGA AAG GG-3′ and 5′-TCC TCA TCA CGC ATC TGT TC-3′ (for *VSVG-PSF2*), 5′-TAC GAT GTT CCA GAT TAC GCG GG-3′ and 5′-CAG GAT GTC GTC CAA AGA CA-3′ (for *HA-PSF3*); 5′-CTC ATC TCA GAA GAG GAT CTG GG-3′ and 5′-GTG TGG TCC ATA TAC TCT TTG-3′ (for *Myc-SLD5*).

Transplantation study

For the analysis of sensitivity of HSCs to 5-FU in vivo, 8-week-old mice were treated with 5-FU (see "Cell culture"), and after 1 day of 5-FU treatment, *PSF1*$^{+/+}$ or *PSF1*$^{+/-}$ BM mononuclear cells (Ly5.2, 4×10^5) were transplanted into lethally irradiated (8.5 Gy) recipients (Ly5.1) together with untreated normal Ly5.1 BM cells (2×10^5). Four weeks after transplantation, donor contribution was determined by FACS using anti-Ly5.1 (eBioscience) and anti-Lin antibodies mixture.

Results

PSF1 is predominantly expressed in proliferating immature hematopoietic cells

Previously, we reported that *PSF1* expression was predominantly observed in immature cell populations in embryonic and adult tissues, such as blastocysts and spermatogonium in the adult.[18] Moreover, *PSF1* expression was observed in immature hematopoietic cells (HCs) designated as Lin$^-$ c-kit$^+$ Sca-1$^+$ (KSL) at the RNA expression level. To confirm whether PSF1 protein is expressed in HSCs or not, CD34$^-$ or CD34$^+$ KSL, Lin$^-$ c-kit$^+$Sca-1$^-$ (KL) or Lin$^+$ cells from adult BM were sorted, and expression of PSF1 was determined in each fraction (Figure 1A). It has been reported that CD34$^-$ KSL cells in the adult mouse BM are dormant and represent HSCs with long-term marrow repopulating ability, whereas CD34$^+$ KSL cells are progenitors with short-term

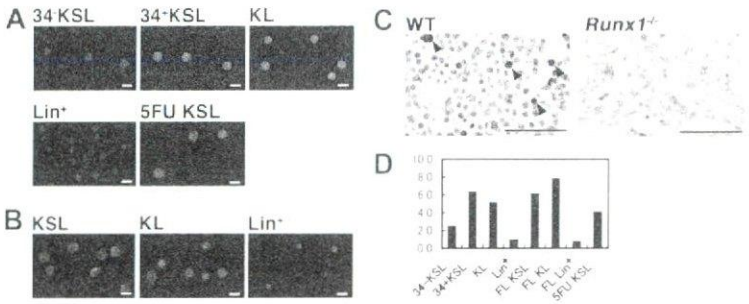

Figure 1. PSF1 expression in proliferating HSC population. (A,B) Immunostaining of several BM (A) or FL-derived (B) HC population with anti-PSF1 antibody. (A) CD34$^-$ KSL (CD34$^-$c-kit$^+$Sca-1$^+$Lin$^-$ cells), 34$^+$KSL (CD34$^+$c-kit$^+$Sca-1$^+$Lin$^-$ cells), KL (c-kit$^+$Sca-1$^-$ Lin$^-$ cells), Lin$^+$ (Lin$^+$ cells), and 5-FU KSL (5-FU-treated mouse derived CD34$^+$KSL cells). (B) KSL (c-kit$^+$Sca-1$^+$Lin$^-$ cells), KL (c-kit$^+$Sca-1$^-$Lin$^-$ cells), and Lin$^+$ (Lin$^+$ cells). Green color shows PSF1 staining. Nuclei were counterstained with PI (red). Bar represents 10 μm. (C) Sections of E12.5 FL from wild-type (WT) or *Runx1*$^{-/-}$ mice were stained with anti-PSF1 polyclonal antibody. Sections were counterstained with hematoxylin (original magnification ×400). Arrows indicate PSF1$^+$ cells. Bars represent 50 μm. (D) *PSF1* mRNA expression in various HC fractions of BM or FL cells as indicated in panel A. 5-FU KSL indicates KSL cells were sorted from BM of mice 4 days after treatment with 5-FU. The values were normalized to the amount of mRNA in Lin$^+$ cells from BM.

reconstitution capacity.[2,24] In the steady state, a high level of PSF1 expression was observed in CD34$^+$ KSL cells and KL cells, whereas a very low level of PSF1 expression was observed in CD34$^-$ KSL cells. However, no PSF1 expression was detected in mature cells (Lin$^+$; Figure 1A). It was reported that, after BM ablation, all HSCs express CD34 in a situation when BM is acutely reconstituted.[25] Therefore, to know whether PSF1 expression in HSCs correlates with cell cycle of HSCs, CD34$^+$ KSL cells were sorted from the BM 4 days after ablation of the BM by 5-FU. As expected, almost all CD34$^+$ KSL cells were stained by anti-PSF1 antibody (Figure 1A).

It is known that HSCs in the FL contain cells that cycle at a higher rate than those in the adult BM and HSCs express the Mac-1 antigen.[26] We sorted KSL (without Mac-1), KL, and Lin$^+$ cells from the FL at embryonic day (E) 12.5 and determined PSF1 expression. High PSF1 expression was found in both KSL and KL cells (Figure 1B), and Lin$^+$ cells did not express PSF1 as seen in the adult BM.

On immunohistochemistry, PSF1 expression was seen in a small population of round HCs in the FL at E12.5 (Figure 1C). However, in the adult liver, which is no longer a hematopoietic organ, PSF1 expression was not observed (data not shown). Furthermore, to test the specificity of this staining in the FL, we studied PSF1 expression in *Runx1*-deficient mice, which lack definitive hematopoiesis[27] and could not detect PSF1-positive cells in the FL in this mutant embryo (Figure 1C). To confirm the specific expression of PSF1 in proliferative and immature HCs, we performed qRT-PCR (Figure 1D). PSF1 was highly expressed in BM-derived CD34$^+$ KSL and Lin$^-$Kit$^+$, and FL-derived Lin$^-$Kit$^+$Sca1$^+$ and Lin$^-$Kit$^+$ cells. KSL cells derived from BM at 4 day after 5-FU treatment also expressed higher amounts of *PSF1* transcript than CD34$^-$ KSL cells. These results demonstrated that PSF1 is highly expressed in proliferating HSCs and progenitors.

Pool size of HSCs/HPCs is decreased in *PSF1*$^{+/-}$ old mice

To investigate how haploinsufficiency of *PSF1* affects hematopoiesis, we analyzed the BM of *PSF1*$^{+/-}$ mice.[18] Although no significant differences were found in KSL cells (Figure 2A) and mature cells populations (data not shown) between wild-type and *PSF1*$^{+/-}$ at 8 weeks of age, the relative number of KSL cells was approximately 2-fold lower in one year-old mice compared with wild-type littermates (Figure 2B). In addition, the population of CD34$^-$ KSL cells (LT-HSCs), CD34$^+$ KSL cells (KSL; ST-HSCs),

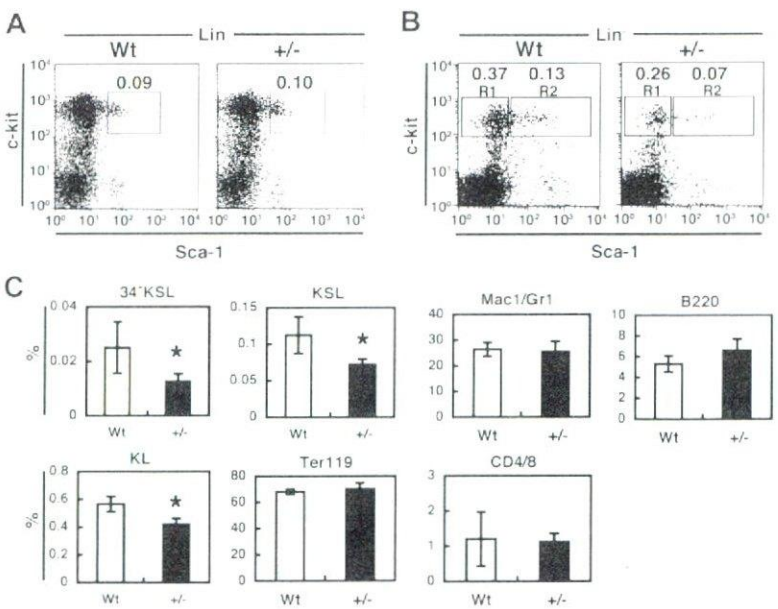

Figure 2. Haploinsufficiency of *PSF1* for hematopoiesis. (A,B) Cells of KSL populations in the BM from 8-week-old mice (A) and 1-year-old mice (B) were analyzed. Percentage of each fraction indicated by box was represented. R1 and R2 in panel B indicates fraction from c-kit$^+$Sca-1$^-$ Lin$^-$ cells and c-kit$^+$Sca-1$^+$Lin$^-$ cells, respectively. (C) Quantitative evaluation in percentage of each fraction among all BM cells of 1-year-old wild-type (Wt) or *PSF1*$^{+/-}$ (+/−) mice as indicated. Mac-1/Gr-1 (myeloid), B220 (B cells), CD4/CD8 (T cells), or TER119 (erythroid). HSCs populations were studied in a CD34$^-$ KSL cell population. Populations of KSL (c-kit$^+$Sca-1$^+$Lin$^-$ cells) and KL (c-kit$^+$Sca-1$^-$ Lin$^-$ cells) were also evaluated. *$P < .05$.

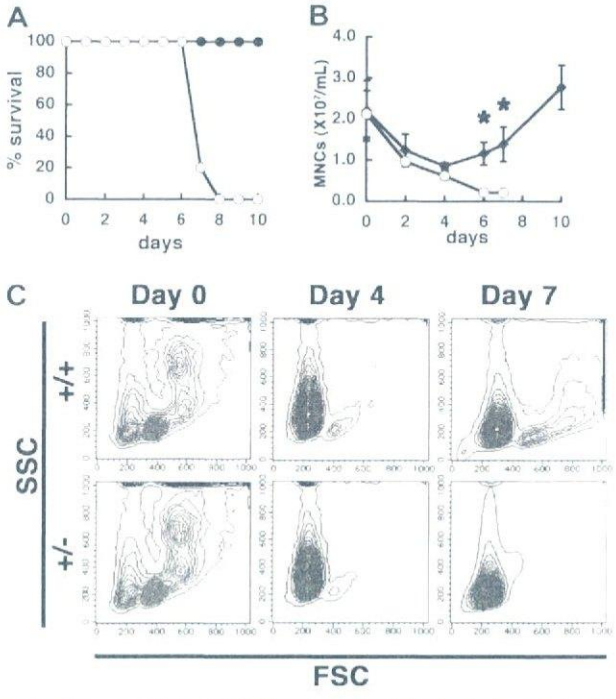

Figure 3. Hypersensitivity of *PSF1*$^{+/-}$ mice to 5-FU. (A) Survival curves after 5-FU injection. ○ indicate *PSF1*$^{+/-}$ 8-week-old mice (n = 10); and ●, wild-type 8-week-old mice (n = 10). (B) Number of mononuclear cells in the peripheral blood of wild-type (●) and *PSF1*$^{+/-}$ (○) mice over time after 5-FU injection. 5-FU was injected into 8-week-old mice on day 0. Means plus or minus SEM are shown (n = 10). *$P < .05$ vs those in PSF1$^{+/-}$ mice on days 2, 4, 6, 8, and 10 after BM ablation with 5-FU. (C) Kinetics of BM cells after 5-FU injection. +/+ indicates wild-type mice; and +/-, *PSF1*$^{+/-}$ mice. Results of FACS analysis are shown. SSC indicates side-scattered light; and FSC, forward-scattered light. Blue represents RBC; and red, leukocytes.

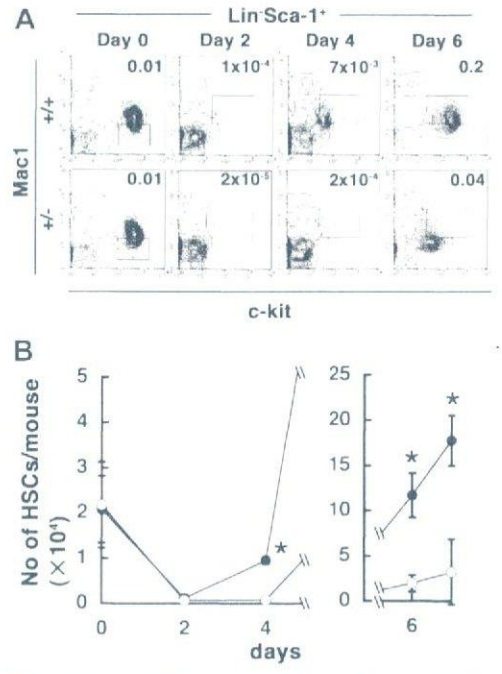

Figure 4. Both alleles of *PSF1* are required for acute reconstitution after BM ablation. (A) Time course of c-kit and Mac-1 expression in Lin$^-$Sca-1$^+$ cells during BM reconstitution after 5-FU injection (+/+, 8-week-old wild-type mice; +/-, 8-week-old *PSF1*$^{+/-}$ mice). Results of FACS analysis are shown. Boxes indicate HSC-containing populations. Percentage of all BM cells corresponding to HSC population indicated by the box is shown in the right corner of each figure. (B) Total number of KSL cells derived from the femurs and tibias of wild-type (●) and *PSF1*$^{+/-}$ mice (○) on the indicated days before (day 0) and after 5-FU injection as described in panel A. *$P < .05$ versus that in *PSF1*$^{+/-}$ mice on the respective day.

and c-kit$^+$Sca-1$^-$Lin$^-$ (KL) were significantly decreased in *PSF1*$^{+/-}$ mice (Figure 2C). The relative cell number of each type of mature HC such as myeloid cells (Mac1/Gr-1$^+$ cells), T cells (CD4/CD8 cells), B cells (B220$^+$), or erythroid cells (TER119$^+$) of the *PSF1*$^{+/-}$ BM was similar to that of the wild-type BM (Figure 2C). These data suggested that both alleles of *PSF1* gene are essential for maintenance of the proper pool size of HSCs or HPCs throughout life.

PSF1$^{+/-}$ mice show hypersensitivity for fluorouracil in the BM

Next, we ablated the BM by 5-FU injection, which kills cycling HSCs/HPCs and forces dormant HSCs into cycle, and studied the ability of *PSF1*$^{+/-}$ mice to reconstitute BM hematopoiesis and analyzed the effect of haploinsufficiency of *PSF1* on HSCs and HPCs (Figure 3A). Although the LD_{50} of 5-FU is 350 mg/kg in normal mice,[28] the *PSF1*$^{+/-}$ mice died within 8 days after a single injection with a lower dose 5-FU (150 mg/kg), whereas wild-type mice did not die with this treatment. On 5-FU injection in *PSF1*$^{+/-}$ mice, the number of peripheral leukocytes decreased precipitously over 7 days; however, in wild-type mice, the number of peripheral leukocytes decreased over 4 days and then it began to increase by day 6 (Figure 3B). After 5-FU injection, the forward scatter$^{dull/high}$ population, which includes lymphocytes, granulocytes, and monocytes, were reconstituted in the BM of wild-type mice after approximately day 7; however, such reconstitution was not observed in the BM of *PSF1*$^{+/-}$ mice (Figure 3C red-colored population). We also calculated the number of peripheral red blood cells and platelets; however, no significant differences were found between *PSF1*$^{+/+}$ and *PSF1*$^{+/-}$ mice in normal and acute phase (data not shown).

PSF1 is essential for HSC proliferation after 5-FU treatment

Before 5-FU injection, there were no obvious differences in the numbers of HSCs and HPCs in the BM between 8-week-old wild-type and *PSF1*$^{+/-}$ mice (Figures 2A, 4A). 5-FU injection induces HSCs into cycle, and it was reported that these cycling HSCs weakly express Mac-1.[26,29] We therefore studied whether 5-FU injection promotes the proliferation of Mac-1^{lo}–expressing HSCs. Before 5-FU injection, the number of HSC population designated as Mac-1$^-$ KSL was not significantly different between wild-type and *PSF1*$^{+/-}$ mice as shown in Figure 2A (see also Figure 4A,B). After 5-FU injection, the KSL cell population decreased in both wild-type and *PSF1*$^{+/-}$ mice during the first few days (Figure 4A). Four to 6 days after 5-FU injection, the population of cycling Mac-1^{lo}–KSL cells increased dramatically in wild-type mice, whereas very few of the KSL cells except for the Mac-1^{lo}–KSL population appeared in the *PSF1*$^{+/-}$ mice (Figure 4A). Because of this delay of recovery, the absolute number of HSCs in the BM was approximately 5.9-fold lower in *PSF1*$^{+/-}$ mice compared with that in wild-type mice at 6 days after 5-FU treatment (Figure 4B).

Loss of PSF1 leads to delayed HSC proliferation in the acute phase after BM ablation

Because it has been reported that the percentage of proliferating HSCs reaches a maximum on approximately day 6 in normal mice,[29] we sorted the total population of HSCs (KSL–Mac-1$^{-/lo}$) and HPCs (Lin$^-$Sca-1$^-$c-kit$^+$Mac-1$^{-/lo}$) on day 6 after 5-FU

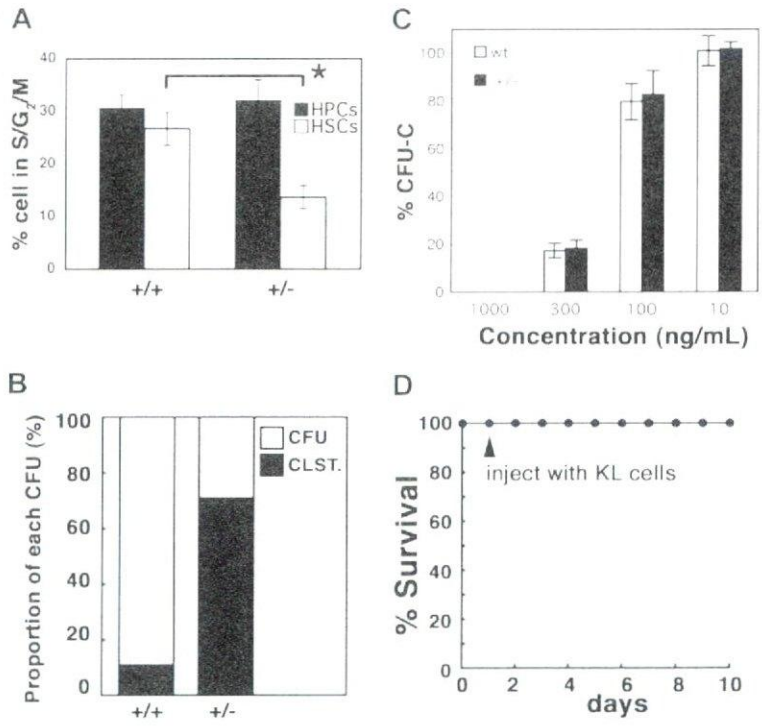

Figure 5. Loss of PSF1 leads to delay of HSC proliferation in the acute phase. (A) Percentage of KSL cells or HPCs (Lin^- c-kit^+ $Sca\text{-}1^-$) in the $S/G_2/M$ phase among the total number of HSCs or HPCs, respectively, on day 6 after 5-FU injection as described in Figure 4A. ■ indicates HPCs; □, KSL cells. Mean values plus or minus SEM are shown (n = 5). *$P < .05$. (B) CFU-c assay using KSL cells obtained from mice on day 6 after 5-FU injection. +/+ indicates wild-type mice; and +/-, $PSF1^{+/-}$ mice. ■ indicates CFU cluster (CLST; containing < 30 cells); □, CFU-C (CFU; containing > 30 cells). (C) Comparison between wild-type and $PSF1^{+/-}$ KSL cells for sensitivity to 5-FU toxicity. Sorted KSL cells from the BM of 8-week-old mice were seeded in semisolid medium with indicated concentration of 5-FU, and total CFU-C number was counted after 10 days of culturing. Results are expressed as a percentage compared with control condition (100%). (D) Rescue experiments. $PSF1^{+/-}$ mice were injected with 5-FU on day 0. One day after 5-FU injection (▲), $Lin^-CD45^+c\text{-}kit^+$ cells (KL cells; 5×10^4/mice) that had been derived from wild-type BM were injected into $PSF1^{+/-}$ mice (n = 5).

injection and analyzed the cell cycle of those HSCs and HPCs. The cells were analyzed for DNA content by PI staining (Figure 5A). The percentage of HSCs in the $S/G_2/M$ phase was approximately 50% lower in $PSF1^{+/-}$ mice than those in wild-type mice, whereas the percentage of HPCs in the $S/G_2/M$ phase was not significantly different between $PSF1^{+/-}$ and wild-type mice. These data suggest that both alleles of *PSF1* are essential for acute BM reconstitution.

When HSCs are cultured in semisolid media, they divide and generate large colonies, including mature HCs. If *PSF1* haploinsufficiency leads to cell death in HSCs, HSCs cannot form colonies in vitro. Therefore, next we investigated the in vitro colony-forming capacity of HSCs (KSL-Mac-$1^{-/lo}$) that had been obtained on day 6 after 5-FU injection by cell sorting (Figure 5B). The HSCs from $PSF1^{+/+}$ and $PSF1^{+/-}$ mice formed the same total numbers of colonies and clusters (data not shown); however, the HSCs from $PSF1^{+/-}$ mice formed a markedly higher number of CFU clusters (> 30 cells) compared with $PSF1^{+/+}$ cells. In the case of HSCs derived from wild-type mice, approximately 89% of all colonies were large colonies; however, approximately 71% of colonies generated by HSCs from $PSF1^{+/-}$ mice were small colonies. To determine whether haploinsufficiency of *PSF1* simply induced cell death resulting in reduced colony size in CFU-c assay, we examined the number of apoptotic cells in the colony-forming cell population by staining with anti–annexin V antibodies (Table 1). No significant differences were found in the apoptotic cells with respect to Lin^-Kit^-, Lin^-Sca1^-, and Lin^- population between cells from CFU-c derived from $PSF1^{+/+}$ and $PSF1^{+/-}$ HSCs. These data suggested that the decreased colony size in $PSF1^{+/-}$ CFU-c is not induced by activation of DNA damage checkpoint and cell death. These results indicated that $PSF1^{+/-}$ HSCs may not easily divide into daughter cells committed to a program of differentiation, but haploinsufficiency did not induce cell death. Furthermore, to test the possibility that $PSF1^{+/-}$ HSCs are simply more sensitive to 5-FU toxicity, KSL cells were sorted from BM of wild-type or $PSF1^{+/-}$ mice and seeded onto semisolid medium in the presence or absence of 5-FU. Figure 5C illustrates the effect of exposure to various concentrations of 5-FU on colony-forming activity of KSL cells. KSL cells survived and those from wild-type and $PSF1^{+/-}$ formed comparable number of colonies, suggesting that deletion of one *PSF1* allele of HSCs does not cause hypersensitivity for 5-FU. To support this interpretation, BM of wild-type or $PSF1^{+/-}$ mice was collected after 1 day of 5-FU treatment and transplanted into lethally irradiated recipient mice together with untreated normal cells as competitor. After 4 weeks of transplantation, donor contribution was determined by FACS. The percentage of contributed cells (chimerism) was 56 plus or minus 12 and 24 plus or minus 14 in recipients, which were transplanted with wild-type or $PSF1^{+/-}$ BM cells, respectively, although the contribution of $PSF1^{+/-}$-derived HSCs in recipient mice was slightly less. These data suggested that deletion of one *PSF1* allele of HSCs does not cause hypersensitivity for 5-FU. Moreover, transplantation of HSCs and HPCs that had been obtained from wild-type mice completely rescued the lethality of 5-FU in $PSF1^{+/-}$ mice (Figure 5D). These data suggest that the defect in acute reconstitution of the BM in $PSF1^{+/-}$ mice is not caused by disruption of the BM microenvironment in these mice.

Table 1. Percentage of apoptotic cells among CFU-c cell population

Marker	Genotype	
	$PSF1^{+/+}$	$PSF1^{+/-}$
Lin^-Kit^+	39 ± 33	36 ± 29
Lin^-Sca1^+	3.6 ± 2.3	2.6 ± 1.6
Lin^-	2.2 ± 1.1	1.8 ± 1.4

It was reported that PSF1 is essential for DNA replication in yeast.[14-17] This observation raises the possibility that haploinsufficiency of *PSF1* leads to abnormal DNA replication, activation of DNA damage checkpoint, S-phase arrest, and cell death in mice. To evaluate this possibility, apoptotic cells were quantified by FACS analysis after staining with annexin V in 5-FU–treated or untreated BM cells (Table 2). In $PSF1^{+/-}$ BM cells, apoptotic cells from Lin^-, Lin^-Kit^+, or $Lin^-Kit^+Sca^+$ cell populations were slightly

Table 2. Percentage of apoptotic cells in various hematopoietic cell populations

Marker	Genotype	
	PSF1$^{+/+}$	PSF1$^{+/-}$
Normal state		
Lin$^-$Kit$^+$Sca1$^+$	5.4 ± 4	9.3 ± 0.4
Lin$^-$Kit$^+$	4.5 ± 3	8.1 ± 0.2
Lin$^-$	7.0 ± 5	12 ± 0.6
5-FU treated*		
Lin$^-$Kit$^+$Sca1$^+$	5.2 ± 2	7.4 ± 0.5
Lin$^-$Kit$^+$	4.2 ± 2	5.1 ± 0.7
Lin$^-$	4.7 ± 2	5.9 ± 1

*BM cells were collected from mice 6 days after treatment with 5-FU.

increased compared with the analogous populations derived from wild-type mice; however, none of these differences was statistically significant. In addition, no obvious S-phase arrest was found in *PSF1*$^{+/-}$ HSCs (Figure 5A). We also examined the expression of ATM, ATR, XCCR1, Brca2, and p21 in both wild-type and *PSF1*$^{+/-}$ CD34-KSL cells by qRT-PCR; however, no obvious differences were found (data not shown). These data suggested that haploinsufficiency does not lead to abnormal DNA replication or increased activation of DNA damage checkpoint.

Taken together, these data indicate that both alleles of *PSF1* are essential for promoting HSC cycling and that this requirement is limited to HSCs.

PSF1 regulates molecular stability of other GINS components in mutual manner

To address whether the silencing of one of the GINS components, PSF1, affects the cellular stability of other GINS components, we performed ectopic expression of all GINS component with or without PSF1 (Figure 6). For the evaluation of the transfection efficiency by plasmids, the amounts of overexpressed gene transcripts were quantified by real-time PCR; no significant differences were found between GINS and G-NS condition for VSVG-PSF2, HA-PSF3, and Myc-SLD5 expression (Table 3). These data indicated that transfection efficiencies of all plasmids were almost equivalent between GINS and G-NS conditions. When all GINS components (PSF1, PSF2, PSF3, and SLD5) were cotransfected, a stable "GINS" complex was formed. However, lack of PSF1 led to destabilization of PSF2, PSF3, and SLD5 (G-NS; Figure 6A). These data suggest that lack of PSF1 results in the formation of an

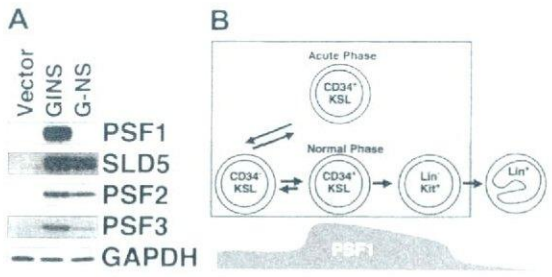

Figure 6. PSF1 mutually regulates molecular stability of other GINS components. (A) Western blot analysis of GINS components ectopically expressed on NIH3T3 cells. Cells were cotransfected with VSVG-PSF2, HA-PSF3, and Myc-SLD5 in the presence (GINS) or absence (G-NS) of Flag-PSF1 or empty vector (Vector). The blots were probed with specific antibodies as indicated. GAPDH was used as a loading control. (B) Scheme of PSF1 expression in the course of HSC differentiation. The level of PSF1 expression is represented by the dark gray area. Both alleles of *PSF1* are essential for populations in the light gray area.

Table 3. Relative mRNA expression in transfected cells

Average of relative expression	Plasmid used for transfection	
	Flag-PSF1, VSVG-PSF2, HA-PSF3, Myc-SLD5 (GINS)	VSVG-PSF2, HA-PSF3, Myc-SLD5 (G-NS)
VSVG-PSF2	1	1.05
HA-PSF3	1	1.14
Myc-SLD5	1	1.14

incomplete GINS complex, along with the destabilization of other GINS components in *PSF1*$^{+/-}$ HSCs. Finally, we concluded that PSF1 is expressed in proliferating HSCs and is essential for BM regeneration and regulation of stem cell pool size (Figure 6B).

Discussion

In this study, we showed that PSF1 is highly expressed in proliferating HSCs, and haploinsufficiency of *PSF1* caused severe delay in induction of HSC proliferation during ablated BM reconstitution and disrupted pool size maintenance of HSCs throughout life. In addition, we showed that PSF1 regulates protein stability of other GINS components.

During embryogenesis, *PSF1*$^{-/-}$ embryos show severe growth defect in the inner cell mass, that is, the pluripotent stem cells.[18] This observation raises the possibility that PSF1 could regulate the proliferation and/or pool size for other tissue stem cells. Recently, stem cells were identified in the small intestine.[30] Crypt base columnar cells are stem cells and can be visualized by continuous bromodeoxyuridine incorporation study. Our preliminary experiment showed that the number of crypt base columnar cells also decreased in adult *PSF1*$^{+/-}$ mice compared with adult wild-type mice (Figure S1, available on the *Blood* website; see the Supplemental Materials link at the top of the online article). Further experiments may help establish the function of PSF1 in the regulation of cell proliferation and/or the pool size of various tissue stem cells.

So far, a multiplicity of molecules have been studied for their role in cell-cycle progression, including extrinsic factors, such as Notch and sonic hedgehog, Wnt3a, etc. and intrinsic factors, such as Bmi1, PTEN, p21, p18, and others.[31] However, the mechanism of DNA replication in HSCs has not been elucidated. Although the essential role of PSF1 in DNA replication has been reported in yeast,[8] its function in mammalian cells has not been clearly understood. We previously reported that *PSF1* was essential for cell division of totipotential embryonic stem cells by gene-targeting studies and showed that *PSF1* was highly expressed in adulthood in BM, testis, and ovary, where cell division of stem cells is actively induced in the adult. Here we reported that PSF1 is essential for acute proliferation of HSCs. Taken together, it is clear that PSF1 plays important roles in cell proliferation of the stem cell system. Moreover, we and other groups isolated mammalian PSF2, PSF3, and SLD5, which together make up the GINS complex, and the roles of these GINS component have been reported in cell division.[7,8] In this report, we found that PSF1 expression was weak in slow cycling CD34$^-$ LT-HSCs and high in cycling CD34$^+$ ST-HSC. Therefore, the GINS complex is likely to closely associate with cell cycle of HSCs. At present, molecules affecting PSF1 expression in dormant HSCs have not been isolated; however, proliferating HSCs after BM ablation by 5-FU almost exclusively express PSF1 at high levels. This suggested that PSF1 expression is

inductively, but not intrinsically, regulated in HSCs affected by exogenous molecules produced from cells responding to BM suppression. At present, although it is not clear whether PSF1 plays a role in DNA replication of HSCs, isolation of molecules affecting PSF1 expression in HSCs may contribute to the understanding of process of self-renewal in HSCs.

It was reported that "GINS" replication complex, which is composed of PSF1, PSF2, PSF3, and SLD5, interacts with CDC45 and MCM complex and is involved in the initiation of DNA replication in lower eukaryote.[14-17] To determine whether haploinsufficiency of *PSF1* impairs DNA replication at stem cell level resulting in reduced pool size of HSCs, we examined the expression levels of DNA-damage checkpoint genes, such as ATM, ATR, XCCR1, BRCA2, and p21 in HSCs. No significant differences were found between $CD34^-$ KSL cells derived from young and old $PSF1^{+/+}$ and $PSF1^{+/-}$ BM (data not shown). These data suggested that the decreased pool size of HSC population in $PSF1^{+/-}$ BM is not induced by activation of DNA damage checkpoint.

In this study, haploinsufficiency of PSF1 severely suppressed BM reconstitution by delaying the proliferation of the HSC population. Based on our result, there are 2 possibilities to explain this suppression not only by gene-dose effect, but also other processes. As one possibility, PSF1 may bring about the molecular stability of DNA replication proteins. Overexpression studies suggested that PSF1 regulates stable expression of other GINS components (Figure 6A). Thus, it is probable that lower expression of PSF1 in HSCs of $PSF1^{+/-}$ mice may lead to down-regulation of SLD5, PSF2, and PSF3 in HSCs. Therefore, incompletely formed GINS complex may have a dominant negative effect and/or induce instability of other DNA replication complexes, such as CDC45 or MCMs. Another possibility is that PSF1 may induce HSC specific gene expression for effective engraftment capacity. It was reported that HSCs shift gene expression and engraftment phenotype with cell cycle transit.[32] Compared with HSCs from wild-type mice, HSCs obtained from 5-FU-injected $PSF1^{+/-}$ mice expressed a lower level of Mac-1, which appeared to be expressed in cycling stem cells and to be involved in cell adhesion (Figure 5A).[26] Thus, haploinsufficiency of *PSF1* may affect HSC properties. As it is thought that DNA replication of important genes for cell function occurs in the early period of the S phase, it is possible that PSF1 regulates the expression of several genes involved in the formation of the BM stem cell niche through DNA replication specifically in HSCs. In addition, loss of PSF1 causes abnormality of chromatin segregation in mice and nematodes (M.U., N.T., unpublished data, May 1, 2007). It has been also reported that PSF2 depletion inhibits the transition of metaphase to anaphase through the suppression of the attachment of tubulin to the kinetochore.[33] These data suggest that the GINS complex might have roles in other biologic processes.

It is also known that, after chemotherapy with anticancer drug, some patients have prolonged BM suppression for unknown reasons.[34] Moreover, BM dysfunction resulting in pancytopenia is observed with aging in elderly people for unknown reasons. Haploinsufficiency of *PSF1* in mice induced delay of BM recovery after 5-FU treatment and attenuated the number of HSCs with aging. Therefore, attenuation of PSF1 expression in HSCs may cause prolonged BM suppression after chemotherapy and pancytopenia with aging. So far, the association of stem cell division with DNA replication proteins in hematopoietic disorders has not been reported. It is intriguing to analyze the relationship of hematopoietic diseases and DNA replication protein, such as PSF1. Based on our analysis, identification of *PSF1*-dependent genes probably sheds light on the mechanism of DNA replication in HSCs and ontogeny of hematopoietic disorders.

Acknowledgments

We thank Dr T. Watanabe (Tohoku University, Japan) for providing us the *AML-1/Runx1* mutant mice, and Ms Y. Shimizu, Ms K. Ishida, Ms M. Sato, Mrs Y. Nakano, Mrs K. Fukuhara, and Mrs N. Fujimoto for technical assistance.

This work was supported in part by the Japanese Ministry of Education, Culture, Sports, Science and Technology and the Japan Society for Promotion of Science.

Authorship

Contribution: M.U. and N.T. designed the research, analyzed data, and wrote the paper; K.S. and M.A. helped generate PSF1 mutant mice; and M.I. helped generate anti-PSF1 antibody.

Conflict-of-interest disclosure: The authors declare no competing financial interests.

Correspondence: Nobuyuki Takakura, Department of Signal Transduction, Research Institute for Microbial Diseases, Osaka University, 3-1 Yamada-oka, Suita, Osaka 565-0871, Japan; e-mail: ntakaku@biken.osaka-u.ac.jp.

References

1. Cheshier SH, Morrison SJ, Liao X, Weissman IL. In vivo proliferation and cell cycle kinetics of long-term self-renewing hematopoietic stem cells. Proc Natl Acad Sci U S A. 1999;96:3120-3125.
2. Osawa M, Hanada K, Hamada H, Nakauchi H. Long-term lymphohematopoietic reconstitution by a single CD34-low/negative hematopoietic stem cell. Science. 1996;273:242-245.
3. Calvi LM, Adams GB, Weibrecht KW, et al. Osteoblastic cells regulate the haematopoietic stem cell niche. Nature. 2003;425:841-846.
4. Reya T, Duncan AW, Ailles L, et al. A role for Wnt signalling in self-renewal of haematopoietic stem cells. Nature. 2003;423:409-414.
5. Varnum-Finney B, Xu L, Brashem-Stein C, et al. Pluripotent, cytokine-dependent, hematopoietic stem cells are immortalized by constitutive Notch1 signaling. Nat Med. 2000;6:1278-1281.
6. Kanemaki M, Sanchez-Diaz A, Gambus A, Labib K. Functional proteomic identification of DNA replication proteins by induced proteolysis in vivo. Nature. 2003;423:720-724.
7. Kubota Y, Takase Y, Komori Y, et al. A novel ring-like complex of Xenopus proteins essential for the initiation of DNA replication. Genes Dev. 2003;17:1141-1152.
8. Takayama Y, Kamimura Y, Okawa M, Muramatsu S, Sugino A, Araki H. GINS, a novel multiprotein complex required for chromosomal DNA replication in budding yeast. Genes Dev. 2003;17:1153-1165.
9. De Falco M, Ferrari E, De Felice M, Rossi M, Hübscher U, Pisani FM. The human GINS complex binds to and specifically stimulates human DNA polymerase alpha-primase. EMBO Rep. 2007;8:99-103.
10. Kamada K, Kubota Y, Arata T, Shindo Y, Hanaoka F. Structure of the human GINS complex and its assembly and functional interface in replication initiation. Nat Struct Mol Biol. 2007;14:388-396.
11. Boskovic J, Coloma J, Aparicio T, et al. Molecular architecture of the human GINS complex. EMBO Rep. 2007;8:678-684.
12. Choi JM, Lim HS, Kim JJ, Song OK, Cho Y. Crystal structure of the human GINS complex. Genes Dev. 2007;21:1316-1321.
13. Chang YP, Wang G, Bermudez V, Hurwitz J, Chen XS. Crystal structure of the GINS complex and functional insights into its role in DNA replication. Proc Natl Acad Sci U S A. 2007;104:12685-12690.
14. Pacek M, Tutter AV, Kubota Y, Takisawa H, Walter JC. Localization of MCM2-7, Cdc45, and GINS to the site of DNA unwinding during eukaryotic DNA replication. Mol Cell. 2006;21:581-587.
15. Bauerschmidt C, Pollok S, Kremmer E, Nasheuer HP, Grosse F. Interactions of human Cdc45 with the Mcm2-7 complex, the GINS complex, and DNA polymerases delta and epsilon during S phase. Genes Cells. 2007;12:745-758.

16. Moyer SE, Lewis PW, Botchan MR. Isolation of the Cdc45/Mcm2-7/GINS (CMG) complex, a candidate for the eukaryotic DNA replication fork helicase. Proc Natl Acad Sci U S A. 2006;103:10236-10241.
17. Gambus A, Jones RC, Sanchez-Diaz A, et al. GINS maintains association of Cdc45 with MCM in replisome progression complexes at eukaryotic DNA replication forks. Nat Cell Biol. 2006;8:358-366.
18. Ueno M, Itoh M, Kong L, Sugihara K, Asano M, Takakura N. PSF1 is essential for early embryogenesis in mice. Mol Cell Biol. 2005;25:10528-10532.
19. Okada H, Watanabe T, Niki M, et al. AML1(−/−) embryos do not express certain hematopoiesis-related gene transcripts including those of the PU.1 gene. Oncogene. 1998;17:2287-2293.
20. Takakura N, Yoshida H, Ogura Y, Kataoka H, Nishikawa S, Nishikawa S. PDGFR alpha expression during mouse embryogenesis: immunolocalization analyzed by whole-mount immunohistostaining using the monoclonal anti-mouse PDGFR alpha antibody APA5. J Histochem Cytochem. 1997;45:883-893.
21. Takakura N, Huang XL, Naruse T, et al. Critical role of the TIE2 endothelial cell receptor in the development of definitive hematopoiesis. Immunity. 1998;9:677-686.
22. Takakura N, Watanabe T, Suenobu S, et al. A role for hematopoietic stem cells in promoting angiogenesis. Cell. 2000;102:199-209.
23. Kong L, Ueno M, Itoh M, Yoshioka K, Takakura N. Identification and characterization of mouse PSF1-binding protein, SLD5. Biochem Biophys Res Commun. 2006;339:1204-1207.
24. Nakauchi H, Takano H, Ema H, Osawa M. Further characterization of CD34-low/negative mouse hematopoietic stem cells. Ann NY Acad Sci. 1999;872:57-70.
25. Tajima F, Deguchi T, Laver JH, Zeng H, Ogawa M. Reciprocal expression of CD38 and CD34 by adult murine hematopoietic stem cells. Blood. 2001;97:2618-2624.
26. Morrison SJ, Hemmati HD, Wandycz AM, Weissman IL. The purification and characterization of fetal liver hematopoietic stem cells. Proc Natl Acad Sci U S A. 1995;92:10302-10306.
27. Okuda T, van Deursen J, Hiebert SW, Grosveld G, Downing JR. AML1, the target of multiple chromosomal translocations in human leukemia, is essential for normal fetal liver hematopoiesis. Cell. 1996;84:321-330.
28. Darnowski JW, Handschumacher RE. Tissue-specific enhancement of uridine utilization and 5-fluorouracil therapy in mice by benzylacyclouridine. Cancer Res. 1985;45:5364-5368.
29. Randall TD, Weissman IL. Phenotypic and functional changes induced at the clonal level in hematopoietic stem cells after 5-fluorouracil treatment. Blood. 1997;89:3596-3606.
30. Barker N, van Es JH, Kuipers J, et al. Identification of stem cells in small intestine and colon by marker gene Lgr5. Nature. 2007;449:1003-1007.
31. Akala OO, Clarke MF. Hematopoietic stem cell self-renewal. Curr Opin Genet Dev. 2006;16:496-501.
32. Lambert JF, Liu M, Colvin GA, et al. Marrow stem cells shift gene expression and engraftment phenotype with cell cycle transit. J Exp Med. 2003;197:1563-1572.
33. Huang HK, Bailis JM, Leverson JD, Gómez EB, Forsburg SL, Hunter T. Suppressors of Bir1p (Survivin) identify roles for the chromosomal passenger protein Pic1p (INCENP) and the replication initiation factor Psf2p in chromosome segregation. Mol Cell Biol. 2005;25:9000-9015.
34. Ulrich CM, Robien K, McLeod HL. Cancer pharmacogenetics: polymorphisms, pathways and beyond. Nat Rev Cancer. 2003;3:912-920.

Published Online First on March 17, 2009 as 10.1158/0008-5472.CAN-08-3490

Research Article

Thyroid Transcription Factor-1 Inhibits Transforming Growth Factor-β–Mediated Epithelial-to-Mesenchymal Transition in Lung Adenocarcinoma Cells

Roy-Akira Saito,[1,2] Tetsuro Watabe,[1] Kana Horiguchi,[1] Tadashi Kohyama,[2] Masao Saitoh,[1] Takahide Nagase,[2] and Kohei Miyazono[1]

[1]Departments of Molecular Pathology and [2]Respiratory Medicine, Graduate School of Medicine, University of Tokyo, Tokyo, Japan

Abstract

Thyroid transcription factor-1 (TTF-1) is expressed in lung cancer, but its functional roles remain unexplored. TTF-1 gene amplification has been discovered in a part of lung adenocarcinomas, and its action as a lineage-specific oncogene is highlighted. Epithelial-to-mesenchymal transition (EMT) is a crucial event for cancer cells to acquire invasive and metastatic phenotypes and can be elicited by transforming growth factor-β (TGF-β). Mesenchymal-to-epithelial transition (MET) is the inverse process of EMT; however, signals that induce MET are largely unknown. Here, we report a novel functional aspect of TTF-1 that inhibits TGF-β–mediated EMT and restores epithelial phenotype in lung adenocarcinoma cells. This effect was accompanied by down-regulation of TGF-β target genes, including presumed regulators of EMT, such as Snail and Slug. Moreover, silencing of TTF-1 enhanced TGF-β–mediated EMT. Thus, TTF-1 can exert a tumor-suppressive effect with abrogation of cellular response to TGF-β and attenuated invasive capacity. We further revealed that TTF-1 down-regulates TGF-β2 production in A549 cells and that TGF-β conversely decreases endogenous TTF-1 expression, suggesting that enhancement of autocrine TGF-β signaling accelerates the decrease of TTF-1 expression and vice versa. These findings delineate potential links between TTF-1 and TGF-β signaling in lung cancer progression through regulation of EMT and MET and suggest that modulation of TTF-1 expression can be a novel therapeutic strategy for treatment of lung adenocarcinoma. [Cancer Res 2009;69(7):OF1–9]

Introduction

Thyroid transcription factor-1 (TTF-1; the product of *NKX2.1* gene), a homeodomain-containing transcription factor, is a master regulator for lung morphogenesis, and TTF-1 null mice die immediately at birth, resulting from profoundly hypoplastic lungs (1). The importance of TTF-1 in human lung homeostasis is also highlighted by the findings that individuals with *TTF-1/NKX2.1* haploinsufficiency exhibit congenital pulmonary disease (2). TTF-1 is mainly expressed in type II pneumocytes and Clara cells and regulates the expression of markers of these cells, i.e., surfactant protein C (SPC) and Clara cell secretory protein (CCSP), respectively (3).

Lung cancer is the most frequent type of cancers and causes death of more than one million people annually. The prognosis remains poor despite the recent advances in chemotherapies and molecular-targeted therapies. Expression of TTF-1 has been shown in all types of lung cancers, but its frequent expression is reported in adenocacinoma (72.1%) and small cell carcinoma (90.5%; ref. 4).

Epithelial-to-mesenchymal transition (EMT) is the differentiation switch directing polarized epithelial cells into mesenchymal cells, which plays key roles during embryonic development (5, 6). Mesenchymal cells arising through EMT significantly contribute to various fibrotic conditions, and the process of tumor cell invasion is also associated with EMT. In addition to the loss of cell-cell adhesions, EMT is characterized by the up-regulation of mesenchymal markers, including fibronectin and N-cadherin, and acquisition of fibroblast-like migratory and invasive phenotypes.

Recent studies revealed that several transcription factors, including Snail, Slug, δEF-1 (ZEB1), and SIP1, are involved in the induction of EMT (7–9). These transcription factors repress expression of E-cadherin and induce EMT when overexpressed in epithelial cells. The inverse process, mesenchymal-to-epithelial transition (MET), has been shown to occur during development and to be perturbed in fibrotic disorders and cancer. In contrast to EMT, however, it is largely unknown as to which signals induce MET.

Transforming growth factor-β (TGF-β) is a multifunctional cytokine that regulates a broad range of cellular responses (10). Three isoforms of TGF-β ligands, i.e., TGF-β1, TGF-β2, and TGF-β3, show different expression profiles in various tissues, including the lung. TGF-β binds to type II and type I serine/threonine kinase receptors and transmits intracellular signals. Smads are the major transducer of TGF-β signaling; Smad2 and Smad3 are phosphorylated by the TGF-β type I receptor and form complexes with Smad4. These complexes accumulate in the nucleus and regulate transcription of target genes. TGF-β suppresses growth of epithelial cells, whereas tumor cells frequently lose the responsiveness to growth inhibitory activity of TGF-β. Moreover, TGF-β is known to promote tumor progression through a diverse repertoire of tumor cell autonomous and host-tumor interactions. TGF-β is the major mediator of EMT and is critically involved in epithelial-mesenchymal interactions during lung morphogenesis (11).

In a model of chronic renal injury, bone morphogenetic protein-7 (BMP-7) has been shown to reverse TGF-β–induced EMT (12), and this finding encouraged us to explore the therapeutic strategy to induce MET in cancer cells, most of which exist in an intermediary phenotypic state of "partial EMT" with the potential to undergo "full EMT." Here, we studied the function of TTF-1 in

Note: Supplementary data for this article are available at Cancer Research Online (http://cancerres.aacrjournals.org/).

Requests for reprints: Kohei Miyazono, Department of Molecular Pathology, Graduate School of Medicine, University of Tokyo, 7-3-1 Hongo, Bunkyo-ku, Tokyo 113-0033, Japan. Phone: 81-3-5841-3345; Fax: 81-3-5841-3354; E-mail: miyazono-ind@umin.ac.jp.

doi:10.1158/0008-5472.CAN-08-3490

lung cancer. Because TTF-1 positivity has been reported to be a good prognostic marker in patients with non–small cell lung cancer (13), we focused on lung adenocarcinoma in the present study. Our results suggest that depletion of TTF-1 in lung adenocarcinoma accelerates the process of EMT, leading to progression of cancer.

Materials and Methods

Reagents and antibodies. TGF-β1 was purchased from R&D Systems and used at the concentration of 1 ng/mL. Anti–phosphorylated Smad2, phosphorylated Smad1/Smad3, fibronectin, and Snail antibodies were from Cell Signaling. Anti–total Smad2/3, N-cadherin, E-cadherin, ZO-1, and CD31 antibodies were from BD Pharmingen (Transduction Laboratories). Anti–TTF-1 antibody was from Lab Vision Corporation. Anti–α-tubulin and pan-cytokeratin antibodies were from Sigma-Aldrich. LY364947 was from Calbiochem and used at the concentration of 3 μmol/L.

Cell lines. A549 and Lewis lung cancer (LLC) cells were from Cell Resource Center for Biomedical Research, Institute of Development, Aging and Cancer, Tohoku University. NCI-H441 (H441) cells were from American Type Culture Collection. LC-2/ad cells were from RIKEN BRC.

Cloning of the human TTF-1 cDNA. There are two alternative transcripts of *TTF-1* gene, and the short form consists of over 90% of total transcripts (14). We cloned open reading frame of the short form from the cDNAs of Lu139 cells.

Phase contrast and fluorescence microscopy. Phalloidin staining and immunocytochemical analyses were carried out, as described previously (15). Fluorescence was examined by a confocal laser scanning microscope (Carl Zeiss). Cells were also photographed using a phase-contrast microscope (Olympus).

Luciferase reporter assay. Human E-cadherin promoter construct was kindly provided by Dr. F. van Roy (Ghent University). Luciferase activity was determined as described previously (15).

Immunoblot analysis. Radioimmunoprecipitation assay buffer and lysis buffer were used for immunoblotting of TTF-1 and other proteins, respectively. Detailed procedures were described previously (16).

RNA isolation and reverse transcription–PCR. Total RNA was isolated with RNeasy (Qiagen), and first-strand cDNA was synthesized using the Superscript First-Strand Synthesis System (Invitrogen). Quantitative reverse transcription–PCR (RT-PCR) analysis was performed using the ABI PRISM 7500 Fast Real-Time PCR System (Applied Biosystems) and Power SYBR Green. The expression level was normalized to that of glyceraldehyde-3-phosphate dehydrogenase. PCR primers are listed in Supplementary Table S1.

Gelatin zymography. The cells infected with Ad-LacZ or Ad-TTF-1 were cultured with serum-free media for 48 h, and the conditioned media were collected. Equal amounts of samples were applied to a 10% (w/v) polyacrylamide gel impregnated with 1 mg/mL gelatin. After electrophoresis, the gel was stained with 0.5% Coomassie blue.

Wound healing and invasion assays. Wound healing assay was performed as described previously (16). Video time-lapse imaging was performed as described in the supplementary information. Images were analyzed using the Image J software (NIH).

Cell invasion assay was performed using a Cell Culture Insert (BD Biosciences). Collagen IC was coated on the upper side of the chamber. Cells were trypsinized and reseeded in each well at a concentration of 5×10^4 per well. After 8 h, the cells on the upper face of the filters were removed, and the cells on the lower surface were fixed in methanol and stained with 0.2% crystal violet and 20% methanol.

RNA interference and oligonucleotides. Transfection of small interfering RNA (siRNA) was performed using HiPerFect reagent (QIAGEN). Human TTF-1 siRNA (Stealth RNAi HSS144278) and negative control (Stealth RNAi 12935-200) were purchased from Invitrogen.

ELISA assay. The culture supernatantnts were acidified with 1 N HCl for 10 min, followed by neutralization with 1.2 N NaOH/0.5 mol/L HEPES. The samples were then subjected to ELISA for TGF-β2 (R&D Systems).

Animal models and statistical analyses. C57/BL6 mice, 5 to 6 wk of age, were obtained from Sankyo Laboratory. A total of 1×10^7 cells in 100 μL of PBS were injected s.c. into mice. Tumor volume was approximated by using the equation, $\text{vol} = (a \times b^2) / 2$, wherein vol is volume, a is the length of the major axis, and b is the length of the minor axis. The results were analyzed statistically by the multivariate ANOVA test using JMP6 software (SAS Institute). Survival was analyzed by Kaplan-Meier method, and P value was calculated by log-rank test. The excised samples were put into OCT compound, frozen in dry-iced acetone, and further sectioned for immunohistochemistry.

Results

Ectopic expression of TTF-1 in lung adenocarcinoma cells. A549 lung adenocarcinoma cells lack TTF-1 expression, whereas H441 cells endogenously express it (17). Adenoviral transduction of TTF-1 (Ad-TTF-1) yielded similar levels of TTF-1 transcripts in A549 cells compared with those in H441 cells infected with control adenoviruses encoding LacZ (Ad-LacZ; Supplementary Fig. S1*A*). TTF-1 was located in the nucleus in A549 cells infected with Ad-TTF-1 (Supplementary Fig. S1*B*), and the known targets of TTF-1, including CCSP and SPC, were induced 96 h after adenoviral transduction (Supplementary Fig. S1*C*).

TTF-1 inhibits EMT in lung adenocarcinoma cells. To study the effects of TTF-1 in lung adenocarcinoma cells, we first examined morphologic changes of A549 cells. TTF-1 caused apparent changes from an elongated shape to a polygonal or round appearance (Fig. 1*A*). Because formation of cell-cell adhesions is mainly dependent on E-cadherin system in epithelial cells, we further explored whether TTF-1 influences E-cadherin expression. Luciferase assay showed that TTF-1 enhances the human E-cadherin promoter activity in a dose-dependent fashion (Fig. 1*B*). Untreated A549 cells lacked E-cadherin expression at low cell density as confirmed by immunocytochemistry. When the cells proliferate to higher cell density, diffuse and weak E-cadherin staining was heterogeneously observed (Fig. 1*C*). Forced expression of TTF-1 resulted in stronger staining of E-cadherin on the cell membrane or in the cytoplasm (Fig. 1*C*, *bottom left*). These findings suggested that TTF-1 might restore the epithelial property, at least partially, and prompted us to explore the effect of TTF-1 on EMT in lung adenocarcinoma cells.

Because TGF-β has been shown to elicit EMT in A549 cells (18), we further investigated the effects of TTF-1 in the presence or absence of TGF-β stimulation. In contrast to untreated A549 cells, TGF-β triggered drastic morphologic changes to a spindle-like or fibroblast-like appearance (Fig. 1*C* and *D*). E-cadherin staining was completely lost in TGF-β–treated cells, regardless of cell density, and actin reorganization was apparent by phalloidin staining, showing the induction of EMT by TGF-β. Interestingly, EMT, induced by TGF-β, was clearly inhibited by ectopic TTF-1 (Fig. 1*C* and *D*).

E-cadherin expression was enhanced by the TGF-β type I receptor inhibitor LY364947 (Supplementary Fig. S2*A*), suggesting that blockade of endogenous TGF-β signaling induces E-cadherin up-regulation. TTF-1 further enhanced E-cadherin expression, in addition to the effect of LY364947 (Supplementary Fig. S2*A*). TTF-1–mediated E-cadherin up-regulation and antagonism to TGF-β–mediated EMT were further confirmed by immunoblotting (Supplementary Fig. S2*B*). Besides loss of E-cadherin, EMT is characterized by up-regulation of mesenchymal markers. TGF-β–mediated up-regulation of fibronectin was antagonized by TTF-1, whereas that of N-cadherin was not significantly affected

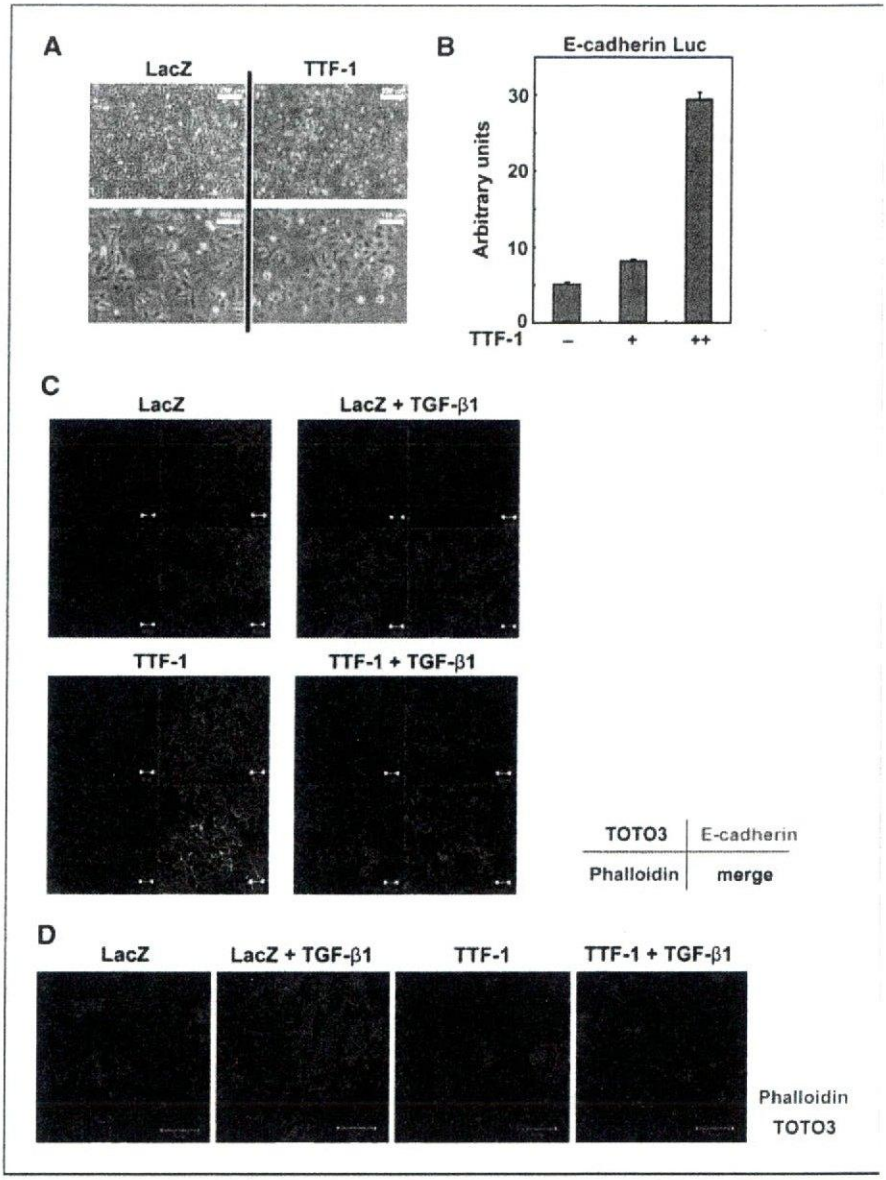

Figure 1. TTF-1 inhibits TGF-β–mediated EMT. *A*, phase contrast microscopy of A549 cells infected with Ad-LacZ or Ad-TTF-1. *B*, luciferase reporter assay of human E-cadherin in A549 cells. *Bars*, SD. *C*, immunocytochemistry for E-cadherin (*green*). *Red*, TRITC-phalloidin; *blue*, TOTO3 (nuclei). A549 cells infected with Ad-LacZ or Ad-TTF-1 for 48 h were incubated with or without TGF-β1 for additional 48 h. *D*, high magnification of the cells treated as in *C*. *Red*, TRITC-phalloidin; *blue*, TOTO3 (nuclei).

(Supplementary Fig. S2*B*). LY364947 suppressed the induction of fibronectin and N-cadherin by TGF-β and up-regulated E-cadherin expression (Supplementary Fig. S2*B*).

In addition to E-cadherin, A549 cells were further immunostained for other epithelial markers, i.e., ZO-1 and pan-cytokeratin (Supplementary Fig. S3). ZO-1 expression was observed in both LacZ-expressing and TTF-1–expressing cells. In LacZ-transduced cells, TGF-β treatment led to the reduction of its staining on the cell membrane, whereas this effect was clearly antagonized by TTF-1. Pan-cytokeratin expression was decreased but sustained even after TGF-β treatment.

TTF-1 attenuates matrix metalloproteinase-2 activity, cell migration, and invasive capacity of lung adenocarcinoma cells. EMT is accompanied with enhancement of matrix metalloproteinase (MMP) activities that facilitate degradation of extracellular matrices surrounding tumor cells. TGF-β treatment enhanced the expression of MMP-2, as determined by quantitative RT-PCR, and this effect was inhibited by TTF-1 (Fig. 2*A*). LY364947 effectively blocked the effect of TGF-β to induce MMP-2 in both of the control and TTF-1–expressing cells (Supplementary Fig. S4*A*). Gelatin zymography further showed that MMP-2 activity was enhanced by TGF-β, and this effect was inhibited by TTF-1 (Fig. 2*B*).

To analyze functional aspects of TGF-β–induced EMT and antagonistic action of TTF-1, we performed wound healing and invasion assays. TGF-β treatment led to highly migratory behavior of cells and earlier closure of wounds after 72 hours, despite of its growth inhibitory action (Fig. 2*C*, *top left*). Expression of TTF-1 resulted in retardation of wound closure reflecting attenuated migratory property, and TGF-β treatment failed to enhance cell migration in TTF-1–transduced cells in contrast to LacZ-transduced cells (Fig. 2*C*, *bottom left*). These effects were quantitated by time-lapse movies (Fig. 2*C*, *right* and Supplementary Videos).

The process of cancer invasion involves the degradation of basement membrane and extracellular matrices that are mainly composed of collagen. To determine the invasive capacity of lung

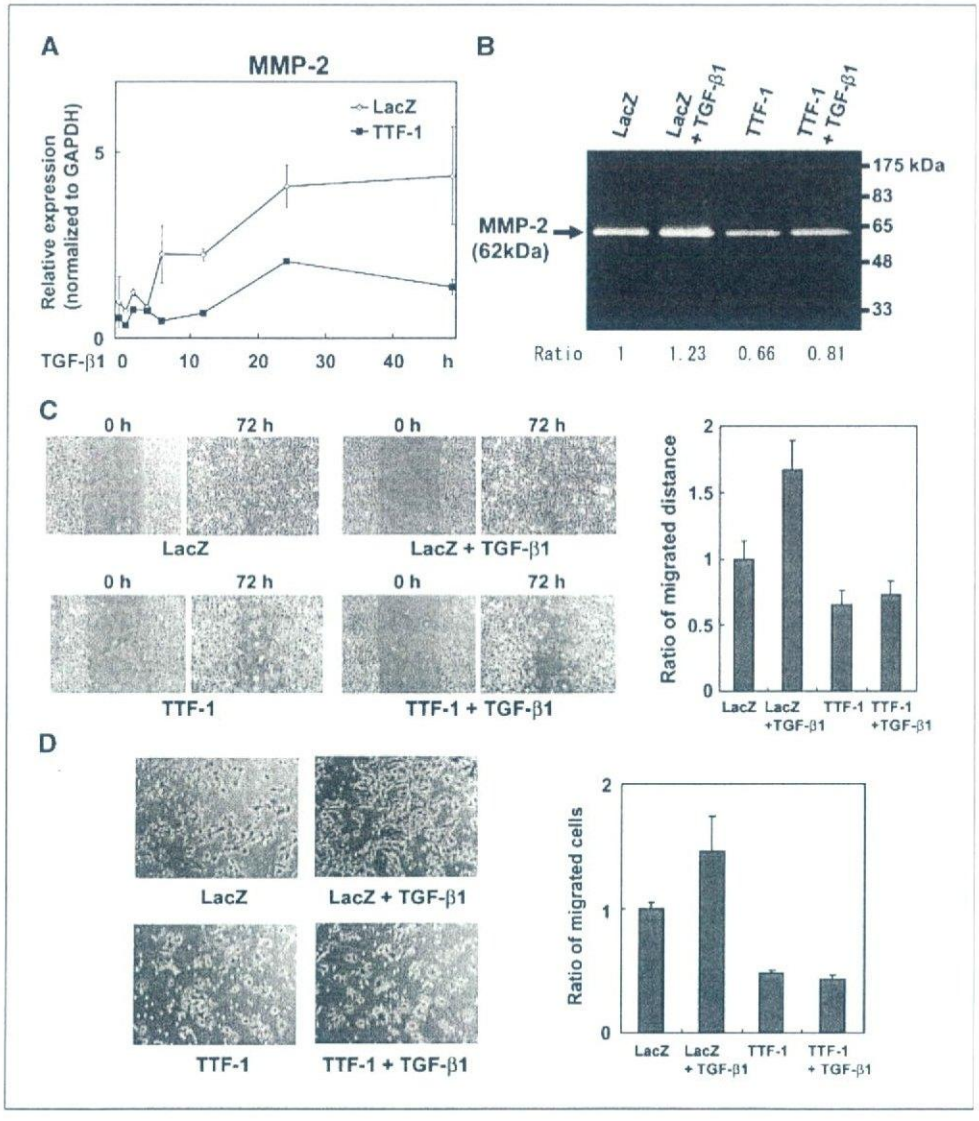

Figure 2. TTF-1 attenuates MMP-2 activity, cell migration, and invasive capacity. *A*, quantitative RT-PCR. Kinetic expression of MMP-2 after TGF-β1 treatment in LacZ-transduced or TTF-1–transduced cells. *Bars*, SD. The values indicate the fold difference compared with 0 h control of LacZ-expressing cells. *B*, gelatin zymography. Gelatin digestion by activated MMP-2 was quantified and relative intensity to control is indicated. Molecular mass markers are in kDa. *C*, *left*, cells infected with Ad-LacZ or Ad-TTF-1 were scratched and incubated with or without TGF-β1 for 72 h; *right*, quantitation of wound healing assay. The distance of cell migration was measured after 24 h by time-lapse video microscopy at eight fields for each group. *Bars*, SD. *D*, *left*, cell invasion assay. The migrated cells were stained with crystal violet. *Right*, quantitation of invasion assay. The migrated cells were counted, and the sum of five random fields was obtained for each well. Each experiment was performed in triplicate. *Bars*, SD.

cancer cells, we used chambers coated with collagen IC. TGF-β treatment resulted in increased number of migrated cells on the lower face of the chambers. TTF-1–expressing cells showed impaired migration through the filters, and the action of TGF-β was completely antagonized by TTF-1 (Fig. 2*D*, *left*). Quantitation of these results revealed that TTF-1 inhibited the invasive capacity of lung adenocarcinoma cells and TGF-β failed to restore it (Fig. 2*D*, *right*).

TTF-1 negatively regulates the expression of molecules involved in EMT. In A549 cells, ectopic TTF-1 inhibited the induction of TGF-β target genes, Smad7 and PAI-1, which are regulated by Smad pathway (Fig. 3*A*). Despite of these striking differences, phosphorylation of Smad2 or Smad3 after TGF-β treatment displayed no significant difference between the control and TTF-1–expressing cells (Supplementary Figs. S5*A* and S5*B*). Next, we knocked down the expression of endogenous TTF-1 in H441 cells. Transfection of TTF-1 siRNA effectively suppressed the expression of TTF-1 (Fig. 3*B*, *left*). TTF-1 knockdown resulted in enhanced induction of Smad7 and PAI-1 after TGF-β stimulation in H441 cells (Fig. 3*B*, *right*), consistent with the results in A549 cells. Recent data have shown that Smad3 physically interacts with TTF-1 and regulates the transcription of the TTF-1 target gene SPB (19, 20). Taken together, it is suggested that TTF-1 suppresses Smad-mediated transcription of a subset of TGF-β target genes in the nucleus and, thereby, inhibits TGF-β–mediated EMT in lung adenocarcinoma cells.

We further explored the antagonistic effects of TTF-1 against TGF-β–induced EMT. Expression of E-cadherin is regulated by multiple transcription factors, including zinc finger transcriptional repressors Snail and Slug (8). TTF-1 suppressed the basal expression level of Snail and Slug, and their rapid induction after TGF-β treatment was also inhibited by TTF-1 (Fig. 3*C*, *left*). Suppressed expression of Snail was also shown by immunoblotting (Fig. 3*C*, *right*). Although LY364947 treatment suppressed the expression of Snail and Slug after 24 h in LacZ-transduced cells, it did not induce further decrease in TTF-1–transduced cells (Supplementary Figs. S4*B* and S4*C*).

Luciferase assay showed that Snail or Slug suppresses the human E-cadherin promoter activity, antagonizing the action of TTF-1 to enhance it (Supplementary Fig. S6*A*). Furthermore, adenoviral

transduction of human Snail resulted in down-regulation of E-cadherin and up-regulation of N-cadherin and fibronectin, mimicking the effect of TGF-β (Supplementary Fig. S6*B*). These results support the idea that Snail and Slug are involved in the regulation of EMT in A549 cells, as previously described in other cell types.

Recently, platelet-derived growth factor (PDGF) signaling (21) and collagen I (22) have been reported to be involved in TGF-β–induced EMT. In A549 cells, TGF-β stimulation resulted in the induction of PDGF-B and α1(I) collagen, whereas this effect was blocked by ectopic TTF-1 (Supplementary Figs. S7*A* and S7*B*). These results suggest that TTF-1 blocks EMT and induces epithelial differentiation by suppression of an array of events leading to EMT. In addition, induction of CTGF after TGF-β treatment was also inhibited by TTF-1 (Supplementary Fig. S7*C*). Thus, it is also suggested that TTF-1 can act as an antifibrotic factor in cancer, as well as in fibrotic disorders, through down-regulation of fibrotic factors.

Silencing of TTF-1 modulates epithelial phenotypes and enhances TGF-β–mediated EMT. To further address the effect of TTF-1 on TGF-β–induced EMT, we knocked down endogenous TTF-1 in H441 cells. Control or TTF-1 siRNA was transfected at 0 and 72 hours in the presence or absence of continuous TGF-β stimulation, and the cell morphology was examined at 144 hours (Fig. 4*A*), because it was previously reported that alveolar epithelial cells undergo EMT when chronically treated with TGF-β for >144 hours (23). Silencing of TTF-1 in H441 cells resulted in morphologic changes to a flattened or elongated shape with decreased cell-cell attachment (Fig. 4*A*). TGF-β treatment led to the reorganization of actin stress fibers, whereas cell-cell adhesions were sustained (Fig. 4*A* and Supplementary Fig. S8*A*). The cells with combined treatment of TTF-1 knockdown and TGF-β showed impaired cell-cell attachment, and fibroblast-like cells were frequently found when cultured at low cell density (Fig. 4*A*, *bottom*).

H441 cells were also immunostained for E-cadherin, ZO-1, and pan-cytokeratin (Supplementary Fig. S8*B*). E-cadherin staining on

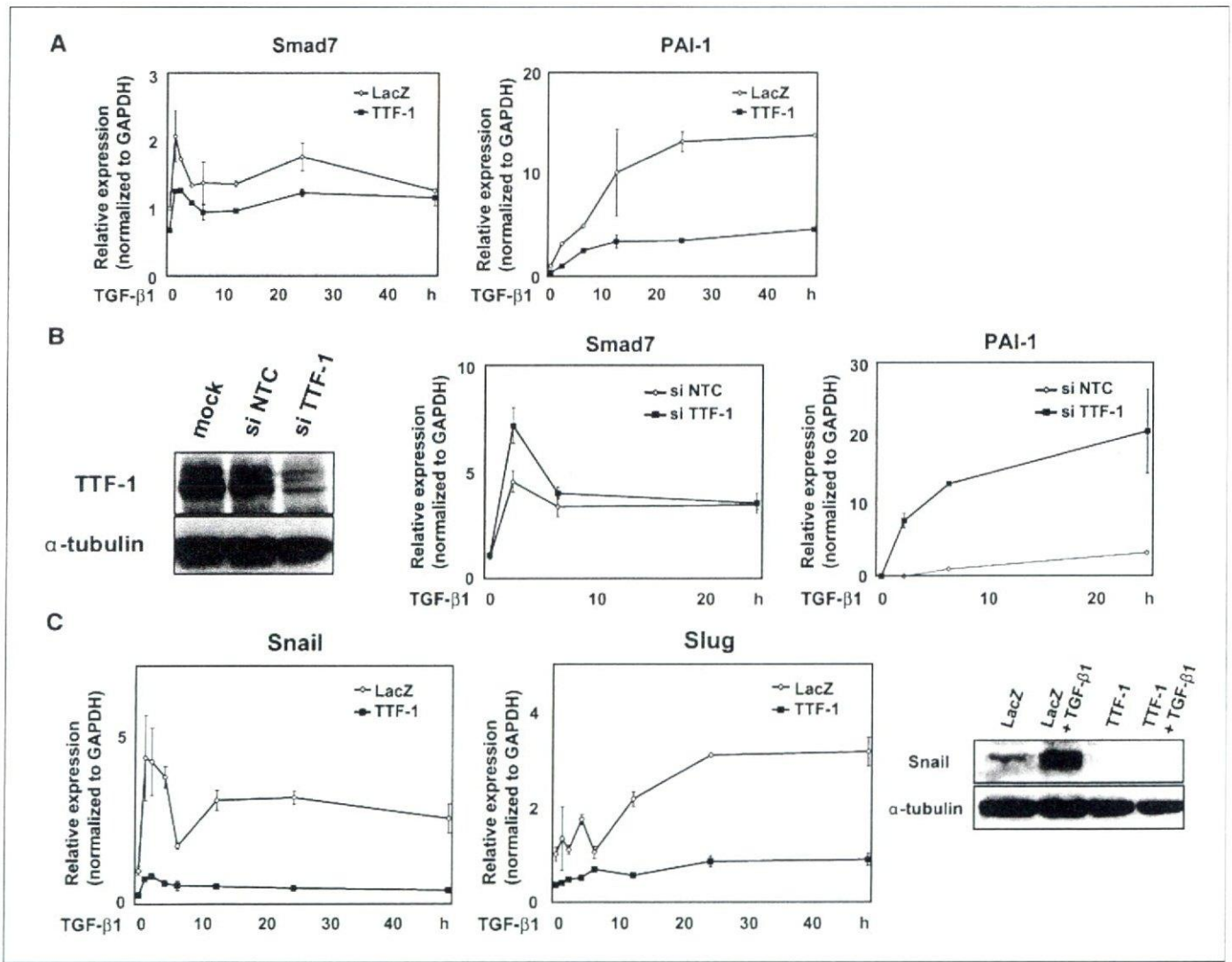

Figure 3. TTF-1 down-regulates the molecules involved in EMT. *A*, quantitative RT-PCR. Kinetic expression of Smad7 and PAI-1 indicated as in Fig. 2*A*. *B*, *left*, immunoblotting of TTF-1 in H441 cells transfected with mock, control siRNA (*si NTC*), and siRNA for TTF-1 (*si TTF-1*). α-Tubulin was used as a loading control. *Right*, quantitative RT-PCR. Kinetic expression of Smad7 and PAI-1. H441 cells were transfected with si NTC or si TTF-1 and treated with TGF-β1 for the indicated time periods. *C*, *left*, quantitative RT-PCR. Kinetic expression of Snail and Slug. *Right*, immunoblotting of Snail in A549 cells infected with Ad-LacZ or Ad-TTF-1 and treated with or without TGF-β1 for 24 h.

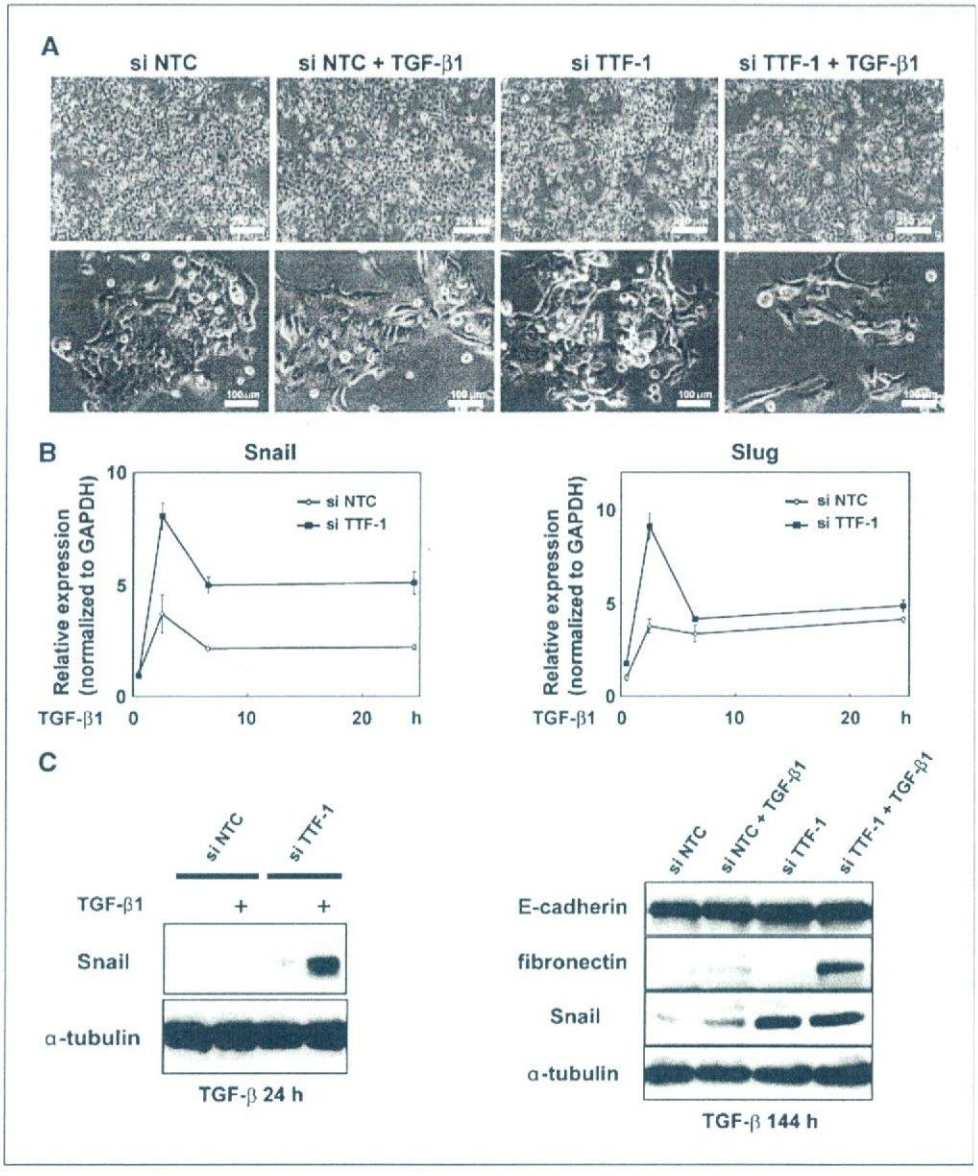

Figure 4. Silencing of TTF-1 enhances TGF-β–mediated EMT. *A*, phase contrast microscopy of H441 cells transfected with si NTC or si TTF-1 and incubated with or without TGF-β1 for 144 h. *B*, quantitative RT-PCR. Kinetic expression of Snail and Slug indicated as in Fig. 3*B*. *C, left*, immunoblotting of Snail in H441 cells transfected with si NTC or si TTF-1 and treated with or without TGF-β1 for 24 h; *right*, immunoblotting of E-cadherin and mesenchymal markers (fibronectin and Snail). H441 cells were transfected with si NTC or si TTF-1 at 0 and 72 h and incubated with or without TGF-β1 for 144 h.

the cell membrane was clearly observed in H441 cells. In contrast to A549 cells, E-cadherin expression was persistent even after TGF-β treatment. TTF-1 knockdown alone failed to significantly suppress its expression, but simultaneous treatment with TGF-β resulted in loss of cell-cell adhesions and substantially decreased E-cadherin staining. Irregular staining of ZO-1 was noted in H441 cells, and TTF-1 knockdown or TGF-β treatment led to its reduced expression. Pan-cytokeratin expression was decreased but sustained even after TGF-β treatment or TTF-1 knockdown. Together with the results in A549 cells, cytokeratins might be persistently expressed in lung cancer cells with mesenchymal phenotypes, consistent with the clinical findings that most lung cancer cells keep expressing cytokeratins.

We next examined the effect of TTF-1 knockdown on both TGF-β–mediated rapid induction of Snail or Slug and expression of EMT markers. Consistent with the observations in A549 cells (Fig. 3*C*), silencing of TTF-1 resulted in enhanced induction of Snail and Slug (Fig. 4*B*). Enhanced induction of Snail was also shown by immunoblotting (Fig. 4*C, left*). We also studied the effect of chronic exposure (144 hours) to TGF-β. TTF-1 knockdown resulted in enhanced expression of Snail, and the induction of fibronectin mediated by TGF-β was enhanced under the condition that TTF-1 was knocked down (Fig. 4*C, right*). These observations support the action of TTF-1, which inhibits EMT mediated by TGF-β. Contrary to the immunocytochemical observations (Supplementary Fig. S8*B*), E-cadherin expression was not significantly affected by either TGF-β treatment or TTF-1 knockdown in a bulk population of the cells cultured at high cell density (Fig. 4*C, right*). This result suggested that E-cadherin expression is retained by other mechanisms that might overcome the effect of TGF-β or TTF-1 in H441 cells cultured at high cell density.

Reciprocal regulation of TTF-1 expression and TGF-β signaling. To address the effect of TGF-β on the expression of TTF-1, we used two different lung adenocarcinoma cell lines, H441 and LC-2/ad, which endogenously express TTF-1. TGF-β treatment for 72 hours suppressed the expression of TTF-1 mRNA and protein

in both cell lines (Fig. 5*A* and *B*), and blockade of TGF-β signaling with LY364947 resulted in restoration of TTF-1 expression suppressed by TGF-β (Fig. 5*B*). These findings were consistent with the previous report, showing reduced expression of TTF-1 in alveolar epithelial cells undergoing EMT (23).

To examine the effect of TTF-1 on the expression of TGF-β ligands, semiquantitative RT-PCR was performed for the three isoforms of TGF-β in A549 cells. Transcription of TGF-β2 was down-regulated by TTF-1, whereas expression levels of TGF-β1 transcripts were not significantly different between the control and the TTF-1–transduced cells (Fig. 5*C*). Transcripts of TGF-β3 were not detected in A549 cells (data not shown). Down-regulation of TGF-β2 expression was further confirmed by quantitation of TGF-β2 protein in the conditioned media (Fig. 5*D*). Taken together, reciprocal regulation between TTF-1 and TGF-β signaling has been observed, suggesting that enhancement of autocrine TGF-β signaling accelerates the decrease of TTF-1 expression and vice versa.

TTF-1 inhibits tumor progression *in vivo*. To address the effect of TTF-1 *in vivo*, we used a mouse syngenic model. Mouse LLC cells stably expressing green fluorescent protein (GFP) or TTF-1 were generated by retroviral gene transfer and were inoculated into syngenic C57/BL6 mice. Retroviral transduction was confirmed by GFP fluorescence (Supplementary Fig. S9*A*). LLCs cells lacked TTF-1 expression, and ectopic TTF-1 was located in the nucleus (Supplementary Fig. S9*B*). Expression of TTF-1 resulted in retardation of tumor growth (Fig. 6*A*), and survival rate was prolonged (Fig. 6*B*). Blood vessel density was lower in the TTF-1–expressing tumor, suggesting that TTF-1 expression might affect tumor-stromal interactions (Fig. 6*C* and *D*).

Discussion

In the present study, we showed that TTF-1 inhibits EMT in response to TGF-β and restores epithelial phenotypes in lung adenocarcinoma cells, leading to suppression of cell migration and invasion. TTF-1 abrogated TGF-β–mediated induction of Snail and Slug, which regulate the changes in gene expression patterns that underlie EMT (9). On the other hand, expression profiles of other factors that have been implicated in EMT, such as δEF-1 (ZEB1) and SIP1 (15), HMGA2 (24), and Twist1 (25), suggested that they are not involved in either TGF-β–mediated EMT or the effect of TTF-1 in A549 cells (data not shown). The mechanism of how TTF-1 inhibits TGF-β–mediated EMT could be explained by multiple mechanisms. One is the suppression of Smad-mediated transcription of EMT-inducing molecules, such as Snail and Slug (Fig. 3), as suggested by the recent findings that Smad3 physically interacts with TTF-1 and regulates its transcriptional activity (19, 20). We have also shown the importance of another pathway; i.e., attenuation of autocrine TGF-β signaling by TGF-β2 down-regulation (Fig. 5).

Accumulating evidence of genomic analyses revealed that TTF-1 gene is amplified in 10% to 15% of lung adenocarcinomas, and *in vitro* studies further support the concept that TTF-1 acts as a lineage-specific oncogene (26–28). On the other hand, the functional significance of TTF-1 in other subsets of lung adenocarcinomas, wherein TTF-1 expression is reduced or lost, still remains to be elucidated.

It is reported that TTF-1 expression is high in well-differentiated carcinomas and relatively low in poorly differentiated carcinomas (13). According to the classification of lung adenocarcinomas into terminal respiratory unit (TRU) type and

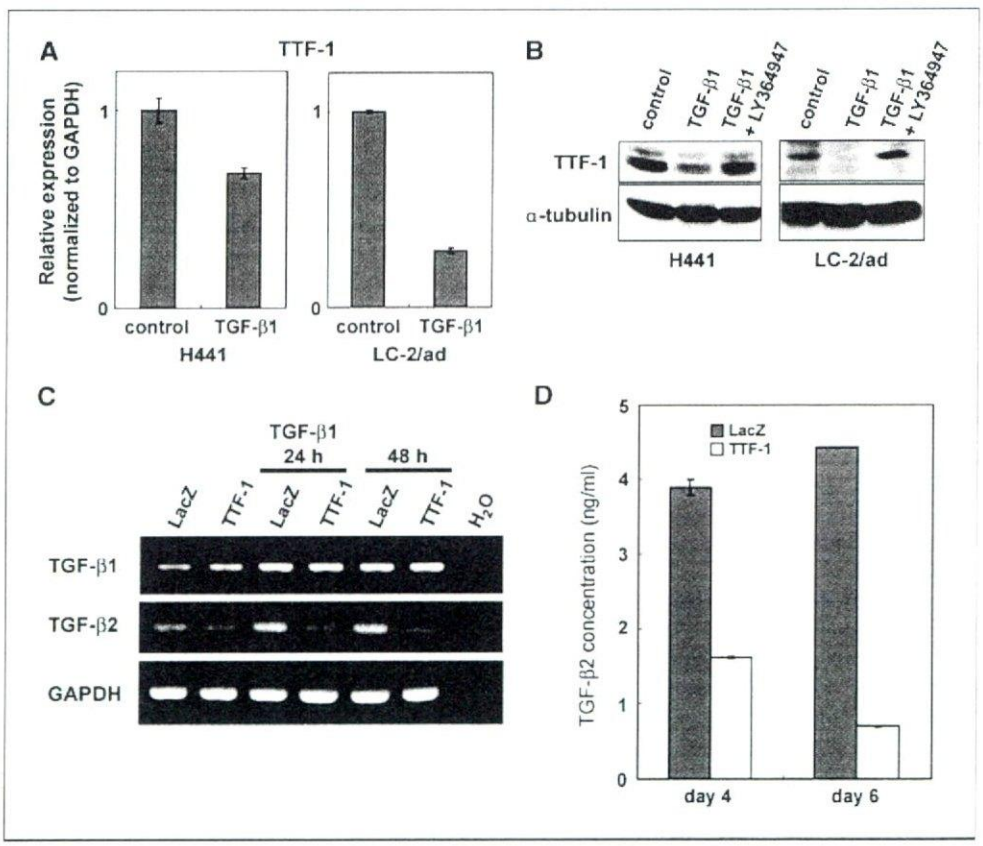

Figure 5. Exogenous TGF-β down-regulates TTF-1 and TTF-1 down-regulates TGF-β2 in lung adenocarcinoma cells. *A*, quantitative PCR of TTF-1. H441 or LC-2/ad cells were treated with or without TGF-β1 for 72 h. *Bars*, SD. *B*, immunoblotting of TTF-1. H441 or LC-2/ad cells were treated with or without TGF-β1 and LY364947 for 72 h. *C*, semiquantitative RT-PCR. A549 cells infected with Ad-LacZ or Ad-TTF-1 were incubated in the presence or absence of TGF-β1 for additional 48 h. *D*, ELISA for TGF-β2. A549 cells infected with Ad-LacZ or Ad-TTF-1 were incubated in serum free media for 48 h (4 d after infection). The cells were incubated for another 48 h in the replaced serum-free media (6 d after infection). *Bars*, SD.

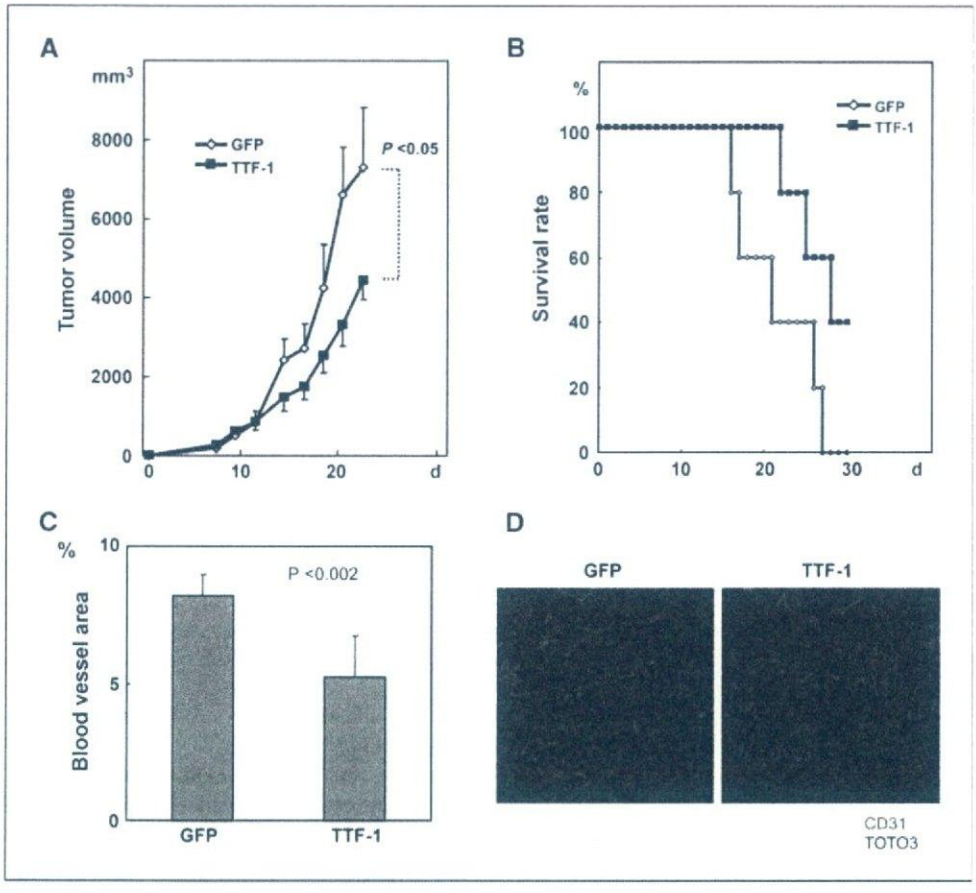

Figure 6. Growth retardation of TTF-1 expressing tumor. *A*, LLC cells infected with retroviruses encoding GFP or TTF-1 were s.c. inoculated into C57/BL6 mice ($n = 5$ for each group). $P < 0.05$ (multivariate ANOVA). *Bars*, SE. *B*, survival rate of the mice bearing GFP-expressing or TTF-1–expressing tumors. $P = 0.068$, log-rank test. *C*, blood vessel density in tumors derived from GFP-expressing or TTF-1–expressing LLC cells. The percentage of the area positively stained for CD31 was measured from randomly selected five fields in each mouse. The value indicates the average of five mice in each group. *P* value was calculated by Student's *t* test. *Bars*, SD. *D*, representative photographs of immunohistochemical staining of CD31 (*red*) in each tumor. *Blue*, TOTO3 (nuclei).

non-TRU type by Yatabe and colleagues, the majority of TTF-1–positive cases showed TRU morphology. Conversely, most of adenocarcinomas with TRU morphology were TTF-1 positive (29). These observations suggest that loss of TTF-1 expression is associated with poor differentiation of adenocarcinomas. Therefore, we believe that recent data showing the oncogenic role of TTF-1 do not exclude the possibility that TTF-1 might act as a tumor suppressor in another subset of lung adenocarcinomas, possibly combined with the mutation or amplification of other oncogenes.

We found that TGF-β suppresses the expression of TTF-1, and this effect was inhibited by LY364947. Expression of TTF-1 might be sustained by the feed-forward mechanism through binding of TTF-1 to its own promoter (30). We have also shown that TTF-1 can attenuate TGF-β signaling by down-regulation of TGF-β2. TGF-β signaling is often positively modulated through the induction of TGF-β ligands of different isoforms (31). Thus, enhancement of autocrine TGF-β signaling may accelerate the decrease of TTF-1 expression, and conversely, TTF-1 may attenuate autocrine TGF-β signaling. Because TTF-1 exerts a tumor suppressive effect through inhibition of EMT, these findings delineate a novel pathway that TGF-β accelerates lung cancer progression.

Three isoforms of TGF-β ligands show different expression profiles during lung branching morphogenesis. Whereas TGF-β1 expression is prominent throughout the mesenchyme, TGF-β2 is mainly localized to the epithelium of the developing distal airways. TGF-β2 may be critical for determining the epithelial cell behavior in a cell autonomous fashion. TTF-1 is expressed at the tip of the developing distal airway and may play a role in the maintenance of the epithelial polarity. Reciprocal regulations between TTF-1 and TGF-β signaling, involved in lung branching morphogenesis, may be recapitulated in lung adenocarcinoma cells.

Loss of TTF-1 expression may be associated with poor differentiation of adenocarcinomas, and our results showed that TTF-1 inhibits EMT and invasiveness of lung adenocarcinoma cells. Some clinical studies showed that TTF-1 positivity is a good prognostic indicator in patients with non–small cell lung cancer. Taken together, our present study sheds light on the new functional aspect of TTF-1, which can inhibit cancer progression.

Disclosure of Potential Conflicts of Interest

No potential conflicts of interest were disclosed.

Acknowledgments

Received 9/8/08; revised 12/25/08; accepted 1/5/09; published OnlineFirst 3/17/09.

Grant support: KAKENHI grants-in-aid for scientific research and Global Center of Excellence Program for "Integrative Life Science Based on the Study of Biosignaling Mechanisms" from the Ministry of Education, Culture, Sports, Science and Technology, Japan.

The costs of publication of this article were defrayed in part by the payment of page charges. This article must therefore be hereby marked *advertisement* in accordance with 18 U.S.C. Section 1734 solely to indicate this fact.

We thank Y. Morishita, C. Iwata, A. Komuro, and T. Shirakihara for technical support and all the members of the Molecular Pathology Laboratory.

References

1. Minoo P, Su G, Drum H, Bringas P, Kimura S. Defects in tracheoesophageal and lung morphogenesis in Nkx2.1$^{-/-}$ mouse embryos. Dev Biol 1999;209:60–71.
2. Krude H, Schütz B, Biebermann H, et al. Choreoathetosis, hypothyroidism, and pulmonary alterations due to human NKX2-1 haploinsufficiency. J Clin Invest 2002; 109:475–80.
3. Minoo P, Hu L, Xing Y, et al. Physical and functional interactions between homeodomain NKX2.1 and winged helix/forkhead FOXA1 in lung epithelial cells. Mol Cell Biol 2007;27:2155–65.
4. Fujita J, Ohtsuki Y, Bandoh S, et al. Expression of thyroid transcription factor-1 in 16 human lung cancer cell lines. Lung Cancer 2003;39:31–6.
5. Derynck R, Akhurst RJ. Differentiation plasticity regulated by TGF-β family proteins in development and disease. Nat Cell Biol 2007;9:1000–4.
6. Thiery JP, Sleeman JP. Complex networks orchestrate epithelial-mesenchymal transitions. Nat Rev Mol Cell Biol 2006;7:131–42.
7. Moustakas A, Heldin CH. Signaling networks guiding epithelial-mesenchymal transitions during embryogenesis and cancer progression. Cancer Sci 2007;98:1512–20.
8. Nieto MA. The Snail superfamily of zinc-finger transcription factors. Nat Rev Mol Cell Biol 2002;3: 155–66.
9. Peinado H, Olmeda D, Cano A. Snail, Zeb and bHLH factors in tumour progression: an alliance against the epithelial phenotype? Nat Rev Cancer 2007;7:415–28.
10. Derynck R, Zhang YE. Smad-dependent and Smad-independent pathways in TGF-β family signalling. Nature 2003;425:577–84.
11. Cardoso WV, Lü J. Regulation of early lung morphogenesis: questions, facts and controversies. Development 2006;133:1611–24.
12. Zeisberg M, Hanai J, Sugimoto H, et al. BMP-7 counteracts TGF-β1-induced epithelial-to-mesenchymal transition and reverses chronic renal injury. Nat Med 2003;9:964–8.
13. Tan D, Li Q, Deeb G, et al. Thyroid transcription factor-1 expression prevalence and its clinical implications in non-small cell lung cancer: a high-throughput tissue microarray and immunohistochemistry study. Hum Pathol 2003;34:597–604.
14. Li C, Cai J, Pan Q, Minoo P. Two functionally distinct forms of NKX2.1 protein are expressed in the pulmonary epithelium. Biochem Biophys Res Commun 2000;270: 462–8.
15. Shirakihara T, Saitoh M, Miyazono K. Differential regulation of epithelial and mesenchymal markers by δEF1 Proteins in epithelial-mesenchymal transition induced by TGF-β. Mol Biol Cell 2007;18:3533–44.
16. Kondo M, Cubillo E, Tobiume K, et al. A role for Id in the regulation of TGF-β-induced epithelial-mesenchymal transdifferentiation. Cell Death Differ 2004;11: 1092–101.
17. Kolla V, Gonzales LW, Gonzales J, et al. Thyroid transcription factor in differentiating type II cells: regulation, isoforms, and target genes. Am J Respir Cell Mol Biol 2007;36:213–25.
18. Kasai H, Allen JT, Mason RM, Kamimura T, Zhang Z. TGF-β1 induces human alveolar epithelial to mesenchymal cell transition [EMT]. Respir Res 2005;6:56.
19. Li C, Zhu NL, Tan RC, Ballard PL, Derynck R, Minoo P. Transforming growth factor-β inhibits pulmonary surfactant protein B gene transcription through SMAD3 interactions with NKX2.1 and HNF-3 transcription factors. J Biol Chem 2002;277:38399–408.
20. Minoo P, Hu L, Zhu N, et al. SMAD3 prevents binding of NKX2.1 and FOXA1 to the SpB promoter through its MH1 and MH2 domains. Nucleic Acid Res 2008;36:179–88.
21. Fischer AN, Fuchs E, Mikula M, Huber H, Beug H, Mikulits W. PDGF essentially links TGF-β signaling to nuclear β-catenin accumulation in hepatocellular carcinoma progression. Oncogene 2007;26:3395–405.
22. Shintani Y, Maeda M, Chaika N, Johnson KR, Wheelock MJ. Collagen I promotes EMT in lung cancer cells via TGF-β3 signaling. Am J Respir Cell Mol Biol 2008;38:95–104.
23. Willis BC, Liebler JM, Luby-Phelps K, et al. Induction of epithelial-mesenchymal transition in alveolar epithelial cells by transforming growth factor-β1. Am J Pathol 2005;166:1321–32.
24. Thuault S, Valcourt U, Petersen M, et al. Transforming growth factor-β employs HMGA2 to elicit epithelial-mesenchymal transition. J Cell Biol 2006;174: 175–83.
25. Yang J, Mani SA, Donaher JL, et al. Twist, a master regulator of morphogenesis, plays an essential role in tumor metastasis. Cell 2004;117:927–39.
26. Kendall J, Liu Q, Bakleh A, et al. Oncogenic cooperation and coamplification of developmental transcription factor genes in lung cancer. Proc Natl Acad Sci U S A 2007;104:16663–8.
27. Tanaka H, Yanagisawa K, Shinjo K, et al. Lineage-specific dependency of lung adenocarcinomas on the lung development regulator TTF-1. Cancer Res 2007;67: 6007–11.
28. Weir BA, Woo MS, Getz G, et al. Characterizing the cancer genome in lung adenocarcinoma. Nature 2007; 450:893–8.
29. Yatabe Y, Mitsudomi T, Takahashi T. TTF-1 expression in pulmonary adenocarcinomas. Am J Surg Pathol 2002;26:767–73.
30. Nakazato M, Endo T, Saito T, Harii N, Onaya T. Transcription of the thyroid transcription factor-1 [TTF-1] gene from a newly defined start site: positive regulation by TTF-1 in the thyroid. Biochem Biophys Res Commun 1997;238:748–52.
31. Miyazono K. Positive and negative regulation of TGF-β signaling. J Cell Sci 2000;113:1101–9.

COUP-TFII regulates the functions of Prox1 in lymphatic endothelial cells through direct interaction

Tomoko Yamazaki, Yasuhiro Yoshimatsu, Yasuyuki Morishita, Kohei Miyazono* and Tetsuro Watabe

Department of Molecular Pathology, Graduate School of Medicine, and the Global Center of Excellence Program for "Integrative Life Science Based on the Study of Biosignaling Mechanisms", University of Tokyo, Bunkyo-ku, Tokyo 113-0033, Japan

During embryonic lymphatic development, Prox1 homeobox transcription factor is expressed in a subset of venous blood vascular endothelial cells (BECs) in which COUP-TFII orphan nuclear receptor is highly expressed. Prox1 induces differentiation of BECs into lymphatic endothelial cells (LECs) by inducing the expression of various LEC markers including vascular endothelial growth factor receptor 3 (VEGFR3). However, the molecular mechanisms of how transcriptional activities of Prox1 are regulated are largely unknown. In the present study, we show that COUP-TFII plays important roles in the regulation of the function of Prox1. In BECs and LECs, Prox1 promotes the proliferation and migration toward VEGF-C by inducing the expression of cyclin E1 and VEGFR3, respectively. Gain-of-function studies showed that COUP-TFII negatively regulates the effects of Prox1 in BECs and LECs whereas loss-of-function studies showed that COUP-TFII negatively and positively regulates Prox1 in BECs and LECs, respectively. We also show that endogenous Prox1 and COUP-TFII physically interact in LECs and that both Prox1 and COUP-TFII bind to the endogenous cyclin E1 promoter. These results suggest that COUP-TFII physically and functionally interact during differentiation and maintenance of lymphatic vessels.

Introduction

Lymphatic vascular systems play critical roles in the maintenance of tissue fluid homeostasis and the mediation of the afferent immune response. Defects in the lymphatic systems result in lymphedema. In pathological situations, they serve as routes of the metastatic spread of malignant tumors to regional lymph nodes. Because of such clinical relevance, understanding of the molecular mechanisms that govern lymphangiogenesis is crucial (Karpanen & Alitalo 2008).

Numerous groups have shown that activation of signaling pathways via vascular endothelial growth factor receptor 3 (VEGFR3) by VEGF-C/D plays central roles in the formation of lymphatic systems. Genetic ablation of *Vegf-c* gene leads to the lack of lymphatic formation (Karkkainen *et al.* 2004). Additionally, expression of VEGF-C under skin-specific promoter induces hyperplasia of cutaneous lymphatic vessels (Jeltsch *et al.* 1997; Veikkola *et al.* 2001). Furthermore, inhibition of VEGFR3 signals via VEGFR3-Fc trap leads to diminishment of lymphatic vessels (He *et al.* 2002).

However, lymphangiogenesis is not regulated only by VEGFR3 signaling pathways. Recent reports have shown that integrin $\alpha 9/\beta 1$ complexes serve as receptors for VEGF-C/D to regulate cell migration (Vlahakis *et al.* 2005). Furthermore, receptor tyrosine kinases including Tie2 (Morisada *et al.* 2005), fibroblast growth factor receptor 3 (FGFR3: Shin *et al.* 2006), platelet-derived growth factor receptor β (PDGFRβ: Cao *et al.* 2004) and hepatocyte growth factor receptor (HGFR: Kajiya *et al.* 2005) have been implicated in lymphangiogenesis. Therefore, if there are transcription factors that regulate these multiple lymphangiogenic signals, such master regulators can be ideal candidates as targets of anti-lymphangiogenesis therapies.

During embryonic lymphatic development, a homeobox transcription factor Prox1 has been shown to play important roles in the differentiation of venous endothelial cells

Communicated by: Masayuki Yamamoto (Tohoku University)
**Correspondence*: miyazono@m.u-tokyo.ac.jp

DOI: 10.1111/j.1365-2443.2008.01279.x

into lymphatic endothelial cells (LECs; Oliver 2004). At 9.5 dpc of mouse development, Prox1 starts to become expressed specifically in a subpopulation of endothelial cells located on one side of the anterior cardinal vein. At this stage, venous endothelial cells express CD34, a blood vascular endothelial cell (BEC) marker, and low level of VEGFR3, whose expression becomes restricted to LEC at later stages. Upon Prox1 expression, expression of BEC markers decreases while expression of LEC markers, such as podoplanin and VEGFR3, increases. These Prox1 expressing cells start sprouting from veins and migrate towards mesenchymal cells expressing VEGF-C. Importantly, in Prox1 deficient mice, the migration of LECs is arrested, leading to complete lack of lymphatic systems (Wigle & Oliver 1999; Wigle *et al.* 2002).

Being a transcription factor, Prox1 regulates the expression of various target genes. When Prox1 was adenovirally transduced into human dermal microvascular endothelial cells (HDMECs), expression of LEC-specific genes was up-regulated (Petrova *et al.* 2002). Although Prox1-mediated induction of LEC-specific genes was not observed in non-BECs, Prox1 was capable of inducing the expression of cyclin E1 and E2 in various cell types. These results suggest that Prox1 may induce cell proliferation and differentiation of BECs into the LECs.

We recently examined the effects of Prox1 on the migration of two types of endothelial cells, mouse embryonic stem cell-derived endothelial cells and human umbilical vein endothelial cells (HUVECs) (Mishima *et al.* 2007). Prox1 induces the expression of VEGFR3 and integrin α9, which results in the endothelial migration towards VEGF-C. Furthermore, when Prox1 expression was knocked-down in human dermal LECs (HDLECs), expression of VEGFR3 and integrin α9 was attenuated with decrease in the migration towards VEGF-C. These results suggest that Prox1 serves as a master regulator in the differentiation and maintenance of LECs.

However, the molecular mechanisms of how Prox1 regulates the transcription of its target genes have been poorly understood. Shin and colleagues showed that Prox1 directly binds to the FGFR3 promoter to induce its expression in endothelial cells (Shin *et al.* 2006). Prox1 has also been shown to bind to the βB1-crystallin promoter to regulate its expression in lens epithelium (Cui *et al.* 2004). While various transcription factors are involved in the regulation of βB1-crystallin expression, the roles of Prox1 binding proteins in the Prox1-mediated transcriptional regulation have not yet been elucidated.

Qin *et al.* showed that Prox1 binds liver receptor homologue-1 (LRH-1/NR5A2), a member of *fushi tarazu* factor 1 subfamily of orphan nuclear receptors, which positively regulates the expression of cholesterol 7-α-hydroxylase (cyp7a1) in liver. Prox1 negatively regulates the transcriptional activities of LRH-1 by sequestrating LRH-1 proteins from cyp7a1 promoter (Qin *et al.* 2004). The suppression of the transcriptional activities of LRH-1 by Prox1 does not require the DNA binding domain of Prox1. These results suggest that other nuclear receptor family members may also physically and functionally interact with Prox1.

Chicken ovalbumin upstream promoter transcription factors (COUP-TFs) are orphan members of the steroid/thyroid hormone receptor superfamily. Two genes termed COUP-TFI (also known as EAR3/NR2F1) and COUP-TFII (also known as ARP-1/NR2F2) are closely related members and are expressed in various organs. COUP-TFs play important roles in the regulation of organogenesis, neurogenesis, and cellular differentiation during embryonic development. In blood vessels, COUP-TFII is specifically expressed in venous but not in arterial endothelium (You *et al.* 2005). Targeted disruption of COUP-TFII in endothelial cells results in the acquisition of arterial characteristics in mutant veins, suggesting that COUP-TFII has a critical role in maintaining vein identity. As lymphatic vessels are originated from veins, ablation of COUP-TFII in endothelial cells causes the decrease in Prox1-expressing cells (Srinivasan *et al.* 2007). However, the roles of COUP-TFII in LECs have not yet been elucidated.

In the present study, we found that COUP-TFII is expressed in LECs. By gain- and loss-of-function analyses, we showed that COUP-TFII suppresses the transcriptional activities of Prox1 to induce VEGFR3 and cyclin E1 in HUVECs, which leads to the inhibition of Prox1-mediated induction of endothelial cell proliferation and migration towards VEGF-C. Interestingly, both gain- and loss-of-function of COUP-TFII in HDLECs suppressed the expression of VEGFR3 and cyclin E1, suggesting that endogenous level of COUP-TFII is required to maintain the characteristics of LECs. Furthermore, we showed that COUP-TFII physically interacts with Prox1 and that both COUP-TFII and Prox1 bind to the cyclin E1 promoter. These results suggest that COUP-TFII regulates the transcriptional activities of Prox1 in LECs via physical interaction.

Results

COUP-TFII is expressed in human LECs

We first studied the expression of COUP-TFII in BECs and LECs using HUVECs and HDLECs by Western blot analysis (Fig. 1A). While COUP-TFII protein was detected in both HUVECs and HDLECs, its expression level was lower in HDLECs, in which Prox1 was expressed.